

Interactive comment on “Seasonal variation of tropospheric bromine monoxide over the Rann of Kutch salt marsh seen from space” by C. Hörmann et al.

Anonymous Referee #1

Received and published: 16 May 2016

We would like to thank Referee #1 for the detailed and helpful comments and suggestions he/she made to improve the quality and clarity of our manuscript.

For reference, the original comments (**black**) are always included below, followed by our response (**blue**). Modifications of the original manuscript (**green**) are indicated in **red**.

Hörmann et al. report seasonal variations of tropospheric BrO abundances over the Rann of Kutch (salt desert/seasonal lake at the border of India and Pakistan) using BrO tropospheric column retrieved using OMI UV measurement during 2005-2014. This is a first attempt to quantify tropospheric BrO over salt lakes using satellite measurements. This study agrees well with the scope of Atmospheric Chemistry and Physics. I recommend this article to be published in ACP given that the following major and minor concerns are addressed.

Major comments:

- 1) Total column BrO retrieval using DOAS (Differential Optical Absorption Spectroscopy) has significant uncertainty depending on selection of fitting window, up to $\approx 50\%$ or higher, which may affect the magnitude of tropospheric column BrO and thus the BrO mass abundance quantified using that column. The tropospheric column BrO and BrO mass abundance is as correct as the magnitude of total column BrO retrieved in the given fitting window, and it should be mentioned in the manuscript (in Sect. 3). In addition, comparing the BrO mass abundances from authors' retrieval and those from the OMBRO operational product (using the same approach) will give a good, solid example to show possible uncertainties in mass abundances calculated from satellite BrO measurements.

We agree with the referee that the uncertainty of the retrieved slant column density depends on the selection of the fit window as thoroughly discussed by Vogel et al. (2015). In addition, the final total (and especially the tropospheric) column density/BrO mass depends on the a-priori assumptions used for the radiative transfer calculations.

We compared the results of our own OMI BrO retrieval at MPIC with those from the NASA OMBRO operational product in order to illustrate the differences as suggested by the referee. The calculation of tropospheric BrO VCDs was therefore applied to the BrO slant columns from the OMBRO product in the very same way as for the SCDs retrieved at MPIC. Mean BrO VCDs were calculated for April (the month with the highest BrO VCDs) and October (close to zero BrO VCDs directly after the monsoon season) for the whole time period 2005-2014. Finally, the resulting BrO VCDs over the Rann area ($22.5\text{--}25.5^\circ\text{N}$, $67.5\text{--}72.5^\circ\text{E}$) were integrated along the longitudinal direction (yielding so called *line densities*) to allow an easy comparison of the results (Figure R1).

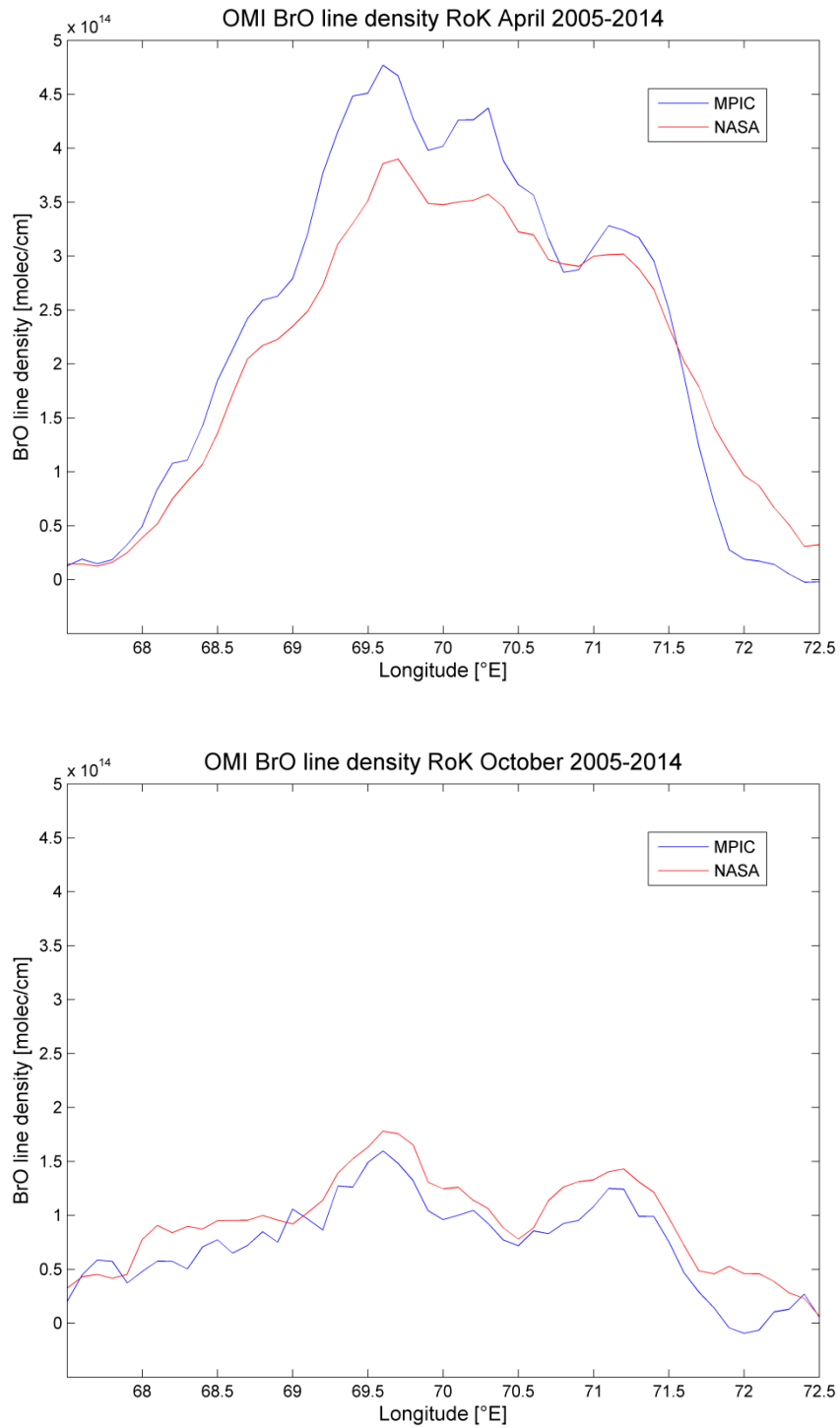


Fig. R1: Comparison of the BrO line densities from the NASA OMBRO product (red) with our (MPIC) evaluation (blue) for April (top panel) and October (bottom panel) of the 2005-2014 period.

As can be seen from Figure R1, the resulting BrO line densities for the MPIC and NASA data are very similar, showing essentially the same features and differences of typically 10%. We added this information to the manuscript at the end of the first paragraph of the “Results” section:

“A detailed comparison of the BrO VCDs with those from the operational NASA OMBRO product showed only small differences of typically 10%. For this purpose, the calculation of troposphere BrO VCDs was applied to the BrO slant columns from the OMBRO product in the very same way as for the SCDs retrieved at MPIC.”

Additional reference:

Vogel, L., Sihler, H., Lampel, J., Wagner, T., and Platt, U.: *Retrieval interval mapping: a tool to visualize the impact of the spectral retrieval range on differential optical absorption spectroscopy evaluations*, Atmos. Meas. Tech., 6, 275-299, doi:10.5194/amt-6-275-2013, 2013.

- 2) Although stratospheric column BrO has little variations at the region of study, the “magnitude” of assumed stratospheric column BrO can affect the magnitude of tropospheric column BrO and thus the magnitude of mass abundances of tropospheric BrO. Such uncertainties in the magnitude are particularly important in this study, since this study aims “quantification” of BrO mass abundances instead of merely tracking the seasonal and temporal variations. How does the estimate of stratospheric column BrO compare with the other estimates using models, such as Theys et al. 2009b and Salawitch et al., 2011? How much can the estimated tropospheric BrO abundances change along with the assumed loadings of stratospheric column BrO? These points need to be addressed in the manuscript (probably in Sect. 3.2).

We agree with the reviewer that a good estimation of the stratospheric BrO column is a prerequisite for the correct quantification of the tropospheric BrO VCD. However, as the enhanced BrO columns over the salt marsh can be expected to be tropospheric (e.g. because of the spatial correlation to the Rann surface), we applied a simple approach to remove the stratospheric BrO contribution by the empirical background correction described in Section 3.2. The advantage of this empirical correction is that it depends on few parameters for the estimation of the stratospheric BrO column and, thus, interferences are effectively avoided. Compared to the spatial extent of the Rann area, stratospheric BrO gradients over the studied area are comparatively small so that they can be modelled/fitted by a simple 2-dimensional (spatial) polynomial.

In order to make this point clearer in the manuscript, we added the following sentences to Section 3.2: “Please note that this rather simple approach can only be applied, because the stratospheric BrO gradients over the studied area are relatively small compared to the extent of the salt marsh. In general, an accurate quantification of tropospheric BrO VCDs (e.g. at high latitudes during arctic spring) needs a more sophisticated estimation of the stratospheric BrO contribution (e.g. Sihler et al., 2012).”

- 3) Sect 4.5: Authors used a geometrical AMF for tropospheric BrO over the Kutch of Rann using GOME-2 data. However, I do not agree with that the BrO column retrieved using nadir-viewing UV measurements and a geometrical AMF over not-so-bright surfaces (albedo ≈ 0.15) has the capability to distinguish tropospheric BrO contribution. If authors cannot prove that using a geometrical AMF has such capability or provide the GOME-2 BrO analysis using tropospheric AMF from reasonable radiative transfer calculation, the entire section need to be removed.

We agree in principle with the referee that a geometrical AMF is not well suited to quantitatively determine the BrO VCD over areas with a relatively low albedo, as a tropospheric BrO enhancement may be underestimated. However, in this subsection, the aim was to perform a qualitative comparison, since for the GOME-2 measurements, the correct calculation of a AMF is hindered by the fact that the GOME-2 cloud product is not

reliable (due to the high surface reflectivity). Also, as mentioned in the beginning of Section 4.5 of the manuscript, the GOME-2 cloud product cannot be used for sorting out measurements that were affected by clouds without losing a significant amount of measurements over the cloud free salt marsh (see also Section 3). Therefore we decided to use geometric AMFs for both satellite instruments in order to ensure a qualitative seasonal intercomparison.

To make this point more clear, we added the following sentence to Section 4.5 of the revised manuscript: “Although geometrical AMFs are not well suited to quantitatively determine the BrO VCD over the Rann, they still can be used to visualize BrO abundances exceeding the comparably smooth stratospheric background.”

Minor comments:

- 1) Latitude and longitude of the Rann of Kutch need to be specified in the early part of the manuscript for readers who are not familiar with the area of study.

We added coordinates at the beginning of Section 1.2 (“...about 22.5-25.5°N, 67.5-72.5°E”)

- 2) Page 2 line 6: “an overall picture of the BrO horizontal distribution” need to be “an overall picture of BrO horizontal distribution in the troposphere” to be clear, since the mentioned satellite measurements of BrO (GOME) primarily provide the total column BrO.

We changed the sentence to:

“In the meantime, an overall picture of the total BrO horizontal distribution was obtained by observations from satellite instruments in the late 1990s (Wagner and Platt, 1998; Richter et al., 1998; Chance, 1998).”

As the referee correctly mentions, the satellite measurements provided just the total column of BrO in the first place.

- 3) Page 2 line 8: Due to the large variations in stratospheric column BrO in high latitudes, polar tropospheric ozone depletion can be identified by satellite measurement only if stratospheric BrO loading is properly addressed, which should be mentioned here.

We changed the sentence to read as follows: “A detailed analysis strongly indicated that the ODEs can be associated with huge tropospheric BrO ‘clouds’ of several thousands of km² extent, ‘(...) rather than by a disturbance of the stratospheric composition or a modification of the stratospheric AMF’ (Wagner and Platt, 1998).”

- 4) Page 6 line 8: “The stratospheric BrO distribution varies little with latitude and even less with longitude (Theys et al., 2009b).” It is the case only for the low latitude regions; stratospheric column BrO has large longitudinal and latitudinal variations in middle and high latitude regions.

We changed the sentence to read as follows: “The stratospheric BrO distribution for lower latitude regions (like the Rann of Kutch area) varies little with latitude and even less with longitude (Theys et al., 2009b).”

Sect 4.3: Choi et al. (2012) have reported the high BrO abundances associated with high planetary boundary layer height in the Arctic region, which can be a relevant reference here.

We changed the beginning of Section 4.3. as follows: “Several studies (e.g. Theys et al., 2009b, Choi et al., 2012, Sihler et al., 2012) discussed the influence of a high boundary layer height on the BrO satellite retrieval over Arctic regions. Recently, Lieb-Lappen and Obbard (2015) analysed the role of blowing snow in the activation of bromine over first-year Antarctic sea ice.”

Interactive comment on “Seasonal variation of tropospheric bromine monoxide over the Rann of Kutch salt marsh seen from space” by C. Hörmann et al.

Anonymous Referee #2

Received and published: 18 May 2016

We would like to thank Referee #2 for the detailed and helpful comments and suggestions he/she made to improve the quality and clarity of our manuscript.

For reference, the original comments (**black**) are always included below, followed by our response (**blue**). Modifications of the original manuscript (**green**) are indicated in **red**.

This manuscript describes measurements of BrO above the Rann of Kutch in India/Pakistan from satellite remote sensing. The work is interesting and well presented, although some use of English should be improved. The scope of the work fits in the journal.

General comments:

The manuscript describes potential albedo effects on the retrieval of tropospheric BrO and tries to argue that albedo is not a contributor to the enhanced BrO observed in this region. That discussion needs further consideration. It is clear from the albedo maps (Fig. 4) that the "white desert" of the Rann of Kutch is higher albedo than surroundings, or during Monsoon is similar to surroundings. The text description indicates that the albedo is lower during the time of the April/May peak, which is true in the sense that of the absolute albedo in the Rann compared to other times of year, but the albedo contrast between the Rann and surrounding areas appears largest during the Feb-May time period. Significantly, the albedo contrast between the Rann and surroundings during the monsoon is very small, so if albedo affects BrO retrieval, no differential albedo exists during the monsoon and no BrO enhancement would be expected. The method of removing a background surrounding the Rann (Eqn. 1 on page 6) is potentially sensitive to the differential albedo between the Rann region and the surroundings. Therefore, I would suggest plotting on Fig. 5 not the reflectivity in the Rann region, but instead the difference in reflectivity between the Rann and the "background" region used for removal of stratospheric BrO influence. At least by eye, this seems to have a pattern more like the BrO enhancement. However, it does appear that the winter season is different than springtime despite similar albedo difference (Rann minus surrounding background regions). That seasonal difference could be affected by stratospheric annual cycling and should be further considered.

The albedo indeed contributes to the BrO enhancement observed over the Rann area and is therefore considered for the radiative transfer calculations (Section 3.3). Nevertheless, the BrO distribution cannot be generally explained by the influence of the bright Rann surface as there is no clear correlation between the observed reflectivity and the BrO VCDs.

The referee correctly notes that the contrast between the Rann and the surroundings changes during the year, not only because of the varying absolute albedo of the salt marsh, but also because of that in the surrounding region. It is therefore very important to make sure that the "differential albedo" does not affect the polynomial stratospheric background correction and (in a worst case scenario) might lead to a spurious enhancement/decrement of the final retrieved BrO VCDs over the Rann.

To minimize this risk, an extensive area surrounding the Rann is used for the stratospheric background correction (18–30°N and 62–78°E; this essentially encompasses the whole area shown in the monthly BrO maps in Figure 3). The actual Rann area (22.5–25.5°N and 67.5–72.5°E) is completely

excluded from the 2D polynomial fit to make sure that the differential albedo between the Rann and the surrounding area doesn't affect this approach.

Following the suggestion of Referee #2 and to further demonstrate that the albedo contrast can not explain the BrO patterns, we normalized the reflectivity of the Rann region by the mean reflectivity in a nearby area (the reference area mentioned in Section 4.2: 22.5-25.5°N/62-67°E) for all months during the time period 2005-2014. To illustrate the change of contrast between Rann and surrounding areas, Figure X1 (right) shows the normalized reflectivity in longitudinal direction over the Great Rann (24°N latitude) along with the increasing BrO VCDs (left) during March-May 2005-2014 (colour coded in blue – March, red – April and black – May). While the BrO VCDs are already enhanced during March, peak in April and clearly decrease and shift towards East in May, it is still obvious from the normalized reflectivity that there is a continuous decrease of the Rann albedo at the same time (please note that the enhanced reflectivity at 67.5°E during May results from increasing cloud coverage at the western coast in the run-up to the monsoon season).

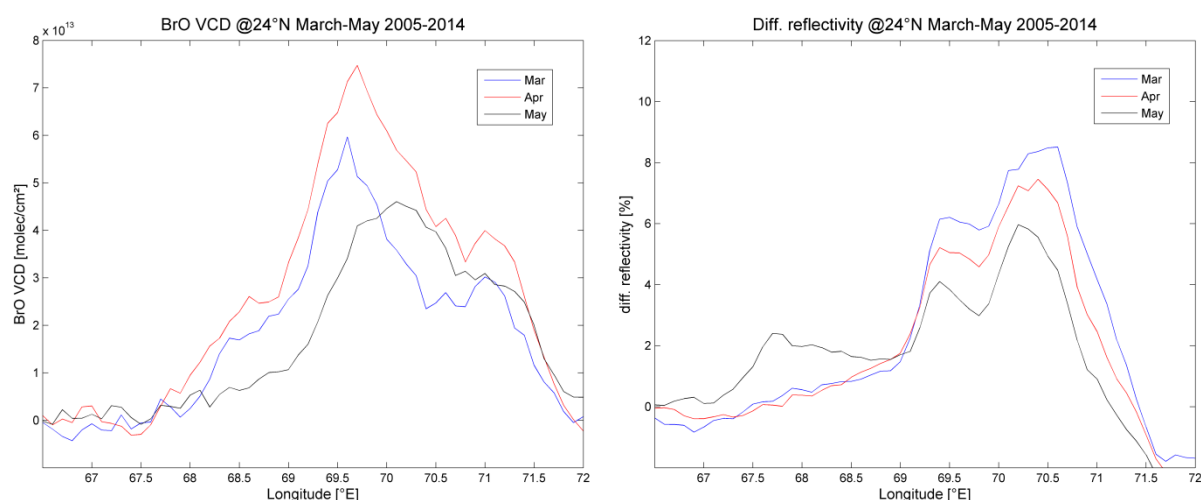


Fig X1: Mean BrO VCD (left panel) and differential reflectivity (right panel) in longitudinal direction over the Great Rann of Kutch at 24°N latitude for March-May (colour coded) 2005-2014.

During winter time (December-February), the differential reflectivity over the Rann (and therefore the contrast between the Indian Ocean and the salt marsh) is even higher, but shows only little variation (Fig. X2, right panel). The corresponding BrO VCDs are only slightly enhanced and also show very small variations, although the upcoming BrO increase seems to already start slowly in February (Fig. X2, left panel).

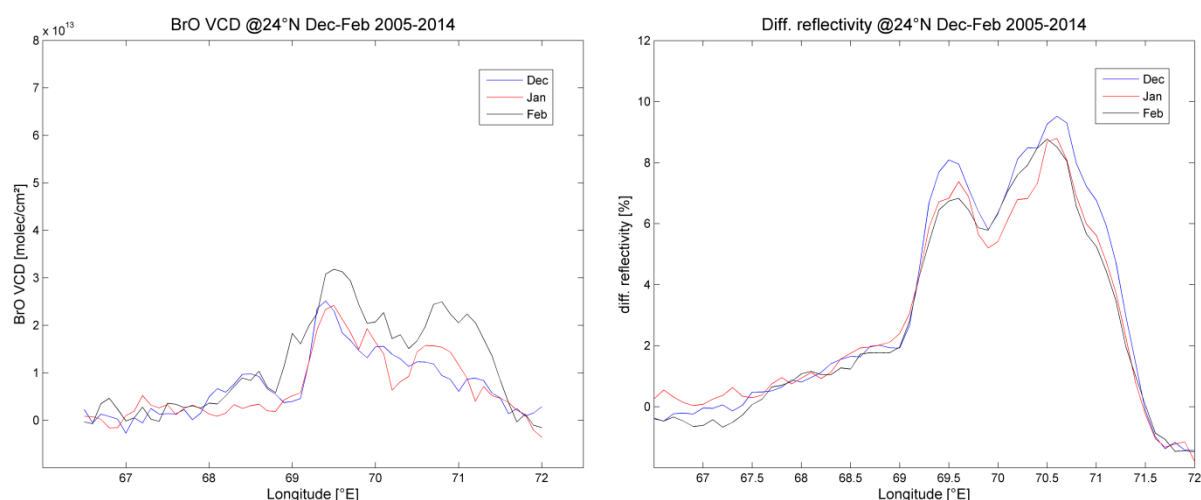


Fig. X2: Mean BrO VCD (left) and differential reflectivity (right) in longitudinal direction over the Great Rann of Kutch at 24°N latitude during December-February 2005-2014 (colour coded in blue – December, red – January and black – February).

Another important finding is that the spatial patterns of the reflectivity and the BrO VCDs are quite different, indicating that the observed enhanced tropospheric BrO VCDs are not a possible artefact caused by the albedo contrast.

We included the results of this accompanying study as an additional section in the Supplementary Material and added the following reference to Section 4.1 of the manuscript:

“While there is only little variation in the regional reflectivity within the Rann area over different months, the spatial distribution of BrO VCDs changes and even seems to progress into the eastern part of the Great Rann from March-May (see Supplementary Material for a more detailed investigation of these effects).”

The discussion of GOME-2 data and comparison to OMI is less well developed than other aspects of the work. A number of arguments are made, but none are really fully explored. For example, there is a discussion of the diurnal cycle of BrO that is indicated to potentially be the cause of lower BrO abundance at the time of GOME-2 overpass (morning) compared to OMI (early afternoon).

We agree with the referee that the discussion of this point is rather qualitative. The reason for this is that the GOME-2 cloud product is not very reliable over the bright surface of the Rann. However, the aim of this study was a relative comparison of both data sets (after they were processed in the same way). We made this more clear in the revised version of the manuscript (see also answer to Referee#1).

At most clean polar sites, BrO cycles are not highly diurnally varying, which is due to production of Br₂ in the prior evening and at night and rapid photolysis of this brown gas in the early morning. Therefore, the supposed cycle at least would differ from polar sites. A reference, Holla et al. (2015), is cited, which does indeed show a peaking of BrO later afternoon. However, the Holla et al. (2015) manuscript also shows NO₂ data that are enhanced through trapping of pollution NO₂ in the shallow nocturnal / early morning boundary layer. Levels of NO₂ above ≈1 nmol/mol appear to prevent production of high BrO levels. Therefore, the diurnal cycle at the Dead Sea may not be appropriate to the Rann of Kutch. In fact, the manuscript doesn't consider regional pollution, when it could have an effect on these data. Nearby Karachi has a population of ≈24 million people, and Ahmadabad is ≈7 million.

We like to thank the reviewer for the valuable note! It is true that the supposed BrO cycle at the Dead Sea in Holla et al. (2015) is often influenced by enhanced levels of NO₂ and therefore differs from those observed in clean polar sites and probably also at the Rann of Kutch. For the Dead Sea, Holla et al. (2015) found mutually exclusive enhanced BrO and NO₂ abundances in time and space, suggesting a conversion of NO₂ into BrONO₂ and therefore suppressing the *bromine explosion* during the early morning. This hypothesis was additionally supported by typically observed diurnal variations of the synoptic winds and meteorology.

In contrast to the Dead Sea area, satellite observations by both considered satellite instruments (OMI and GOME-2) over the Rann of Kutch only show a very localized NO₂ enhancement close to the cities of Karachi (≈ 300-400 km away) and Ahmadabad (≈ 200-300 km away) due to the short NO₂ lifetime of several hours. Close to the salt marsh, the observed tropospheric NO₂ VCDs are typically close to background levels. A possible influence of NO₂ at the Rann of Kutch can therefore expected to be much less important than over the Dead Sea basin. For corresponding tropospheric NO₂ maps for OMI and GOME-2, please visit e.g. the TEMIS website (available via http://www.temis.nl/airpollution/no2col/no2regioomimonth_v2.php).

We revised argument #3 of Section 4.5 as follows:

“3. One of the main chemical reasons for much lower BrO VCDs using GOME-2 might be that the measurements take place about 4 hours earlier when compared to OMI observations (\approx 9:30 vs. 13:30 LT). At the time of the morning overpass, the ‘bromine explosion’ mechanism has presumably not progressed very far, as solar irradiance is approximately 50% less than during OMI’s afternoon overpass (according to ECMWF data) and the process is photolytically driven. Furthermore, O_3 is needed for the rapid build-up of BrO, which might be more easily available during the morning on the one hand, but may lead to differences in the spatial BrO distribution patterns for GOME-2 when compared to OMI. Observations at the Dead Sea (Israel) have shown that the largest BrO VCDs may show up close to noontime, if enhanced NO_x levels are generally present due to anthropogenic pollution (Holla et al., 2015). In contrast to the Dead Sea area, however, neither OMI nor GOME-2 observations show significantly enhanced NO_2 VCDs over the Rann of Kutch area, but only in the vicinity of the cities Karachi (\approx 300-400 km away) and Ahmadabad (\approx 200-300 km away). A possible influence of NO_2 at the Rann of Kutch is therefore assumed to be much less important than over the Dead Sea.”

Other effects like boundary layer height, morning fog/clouds, etc. should be fully discussed and this section should be revised accordingly.

The possible effects of the BLH are briefly discussed on p.13, argument #4, while an influence of clouds (and/or morning fog) due to the different overflight time of the instruments could not be explained from MODIS and ECMWF data (as mentioned in Section 4.5). Furthermore, we are convinced that the best way to conduct such an analysis would be an extensive ground-based local measurement campaign, where the environmental parameters may be observed with much better temporal resolution during the day at the same time as the BrO (and possibly NO_2) column.

To emphasize this, we modified the end of Section 4.5 as follows:

“Although all of these effects probably contribute to the observed differences between OMI and GOME-2 observations, the reasons for these discrepancies are still a matter of further research. The best way to analyze the influence of ambient conditions on BrO formation would be an extensive ground-based measurement campaign. Such local observations would provide high temporal resolution data of meteorological parameters like wind speed and direction, relative humidity, boundary layer height, clouds (and morning fog) as well as a possible influence of anthropogenic pollution.”

The boundary layer height is not treated consistently in this manuscript. In the section about GOME-2 data, 2km (GOME-2 overpass) and 3km (OMI overpass time) are quoted, but the Table 1 and AMF calculations appear to use a 1km ABL height, with alternatives of 0.4 and 2.0 km. This is not consistent and clearly from the sensitivity testing in Table 1, would change the peak BrO mixing ratio significantly.

The referee is right that (according to the ECMWF data) the boundary layer height during the overflight times of the satellite instruments is 2 and 3 km (GOME-2 and OMI), respectively, which may lead to differences of the BrO layer profile and therefore the true BrO VCD. However, the BrO VCDs in [Section 4.5](#) are only calculated by using a geometrical AMF for both instruments (GOME-2 and OMI), which means that neither a specific BrO layer profile nor the boundary layer height is taken into account for the AMF calculation. A more sophisticated AMF calculation for the GOME-2/OMI section remains difficult due to problems with the GOME-2 operational cloud product (see former discussion), so we decided to only show a qualitative comparison of the data. However, a different treatment of GOME-2 and OMI data by assuming BrO layer heights of 2km respectively 3km would result in only about 15 % differences for the resulting BrO VCDs and cannot explain the GOME-2 BrO VCDs close to background level.

It is furthermore important to note that while it can be expected that a change of the boundary layer height may lead to changes of the BrO layer profile, the true BrO profile over the Rann remains unknown (the BrO layer doesn’t necessarily need to fit the boundary layer height). The presumed

baseline scenario (homogeneous BrO layer between 0-1km) only represents a first guess of the true BrO profile, based on the assumption that BrO forms at the salt surface and is partly transported to higher altitudes. To indicate the large uncertainties of the derived BrO mixing ratios, Table 1 shows results for two other a priori BrO profiles. However, for an adequate estimation of the true BrO profile, results from local ground-based MAX-DOAS measurements are desirable.

To emphasize the assumptions made, we modified the manuscript as follows:

Section 3.3 (end): “It is furthermore important to note that the baseline scenario (assuming a homogeneous BrO layer between 0-1km) only represents a first guess of the true BrO profile, based on the assumption that BrO forms at the salt surface and is partly transported to higher altitudes. While the BrO profile can be expected to depend on the prevailing boundary layer height, the true profile over the Rann remains unknown (the BrO layer doesn’t necessarily need to fill in the complete boundary layer). An estimate of the uncertainties caused by the a priori assumptions will be given in Section 4.2. For an adequate estimation of the true BrO profile, however, results from local ground-based MAX-DOAS measurements would be desirable in the future.”

Section 4.5 (argument #4): “4. The boundary layer height during the GOME-2 overflight in April/May is significantly lower ($\approx 2\text{km}$) than for the OMI measurements ($\approx 3\text{km}$). As the BLH increases towards noon, BrO originating from the ground might be transported to higher altitudes where it could be more easily detected by the OMI as the instrument’s sensitivity generally increases for elevated layers. Additionally, the increasing BLH might lead to an increased mixing-in of tropospheric O_3 from higher altitudes and thereby lead to further formation of BrO. It is important to note that the data shown in Figure 4 were only calculated by application of a geometrical AMF and therefore possible differences for the BLH and BrO profile are not taken into account. However, in the case of a homogeneous BrO layer filling in the complete boundary layer, corresponding radiative transfer effects would only result in about 15% differences for the resulting BrO VCDs and can therefore not explain the GOME-2 BrO VCDs close to background level.”

The manuscript should indicate that this work is motivation for measuring BrO from the ground in this region to verify the space-borne observations. Although the region is clearly remote, it is not inaccessible, nor would measurements via simple MAX-DOAS systems be difficult. Verifying the presence or absence of this space-detected feature would significantly contribute to our ability to connect space-based measurements to ground truth.

We totally agree with the referee and modified the manuscript as specified in our answers to the previous comments.

A number of sections discuss that the Rann of Kutch “...is probably one of the strongest natural point sources of reactive bromine...”, but there is no comparison of this source to other sources. Additionally, the manuscript indicates that there is “supposed to have significant impact on local and regional ozone chemistry”, but there is no calculation showing that this impact is significant. It certainly “may” have an impact, but in the absence of some reference indicating significance, the wording appears inaccurate.

We agree with the referee that it is important to emphasize that there are still only few measurements of halogen formation over salt lakes worldwide. To our knowledge, these are the first reported observations of BrO over a salt lake (salt marsh) by a satellite instrument at all. However, there are at least two main points, why the Rann of Kutch is “...probably one of the strongest natural point sources of reactive bromine...” and halogen emissions from salt lakes may “...have significant impact on local and regional ozone chemistry”:

1. By looking at global BrO maps using OMI data, the Rann of Kutch appears to be the only salt lake/marsh where a clear enhancement of the BrO column can be easily seen during several months from satellite measurements, even without correcting for the stratospheric background and excluding clouded data.
2. Although the actual BrO profile over the Rann of Kutch is unknown, a qualitative comparison to the BrO VCDs over the Dead Sea indicates that the BrO abundance over the Rann of Kutch is much larger than over the Dead Sea. So far, the largest BrO mixing ratios at a salt lake were reported from ground-based DOAS measurements at the Dead Sea (up to 220 ppt, as reported in Matveev et al., 2001 and Tas et al., 2005).
It is nevertheless likely that the BrO VCDs over the Rann of Kutch (as well as the Dead Sea) are generally biased low because of spectral dilution due to the low spatial resolution of satellite instruments like OMI when compared to local ground-based measurements (compare to argument #1 of the GOME-2 discussion on p.13 of the revised manuscript).

Saiz-Lopez and von Glasow (2012) state that about 2.5% of the global land surface “(...) is covered by saline soils, implying that halogen release might be relevant on a rather large part of the continents and not only over the comparatively small areas of salt lakes”. However, they also noted that “A regional or global assessment of the relevance of halogen chemistry over salt lakes and saline soils is so far missing”. To further classify the significance of the BrO abundance in comparison to other salt lakes, local ground-based MAX-DOAS measurements are highly desirable (as mentioned several times before).

We added a short paragraph to Section 4.6 of the manuscript to strengthen the given statements as follows:

“It is interesting to note that the BrO VCDs found over the Dead Sea are generally much lower than those observed over the Rann of Kutch, although the above-mentioned ground-based measurements showed the highest BrO mixing ratios so far observed at a salt lake (up to 220 ppt). This finding indicates that the Rann of Kutch is likely one of the strongest natural point sources of reactive bromine compounds outside the polar regions. This argument is further strengthened by the fact that the Rann is the only salt lake/marsh, where a clear enhancement of the BrO column can be easily seen during several months from satellite measurements (even without correcting for the stratospheric background or excluding clouded data). However, BrO from other salt lakes (particularly smaller ones, like the Dead Sea) may generally not be identified as easily from the OMI data.”

Specific comments:

page 1, line 11: indicate that the times are "respectively" **done**

page 1, line 13: replace "former" with "prior" **done**

page 1, line 15: reword "supposed to have a significant influence"

We reformulated the sentence: “The measurements indicate that the Rann of Kutch salt marsh is one of the strongest natural point sources of reactive bromine compounds outside the polar regions.”

page 1, line 19: Missing "von" from "von Glasow" **done**

page 1, line 21: move "significantly" to after "troposphere" [done](#)

page 2, line 19: cut the word "ever" [done](#)

page 2, line 27: are both BrO and IO below 2 ppt? clarify

We reformulated the sentence as follows: "However, none of these measurements showed significantly enhanced BrO or iodine oxide (both less than 2 ppt or below the detection limit of the MAX-DOAS measurements)."

page 4, BrO retrieval: This section appears to indicate that Level 1 OMI data were reanalysed by this group rather than use of the OMI BrO product (OMBRO). Can this be made more clear, and the specific sources of the data from OMI data streams should be described fully. If this calculation differs significantly from OMBRO, that should be noted – why was OMBRO not used?

Our group has a long-standing experience in spectral retrievals of satellite observations, and was one of the first to analyse BrO from satellite. Thus in this study we applied our own algorithm for the analysis of the satellite data (OMI and GOME-2). As shown in the reply to Referee #1, almost the same results are obtained if the OMBRO product is used. We added this information to the text:

The spectral data of both satellite instruments were analysed at MPI-C for BrO column densities by using the Differential Optical Absorption Spectroscopy (DOAS) technique....

The OMI BrO retrieval follows the general settings of the GOME-2 retrieval: Level 1 data (online provided by the Goddard Earth Sciences Data & Information Services center, NASA) were analysed using a wavelength range from 336–360 nm, including 4 adjacent BrO absorption bands.

page 6, line 15: This section is not fully clear. Why are slant columns of BrO (S^*_{trop}) being calculated? Which "geometrical AMF"? Doesn't a geometrical AMF assume that the reflector is the Earth's surface, while the actual tropospheric return may be from clouds / fogs / aerosol light scattering?

A geometrical AMF indeed assumes that the detected sunlight directly traversed the complete atmosphere and is reflected by the Earth's surface alone. However, if the main absorber can be assumed to be mainly present in the stratosphere, the geometrical AMF is a viable approximation for the actual AMF. In the manuscript, the geometrical AMF is solely used for an initial calculation of the main effect of the satellite's measurement geometry and the stratospheric BrO background correction. Please additionally see our answer to Referee #1. We made this point now more clear in the manuscript.

page 6, Radiative transfer section. This seems like it should use at least 2km layer

[Please see comments above](#)

page 6, line 28: "...and briefly described in Carn..." [done](#)

page 7, line 25: Effects of local pollution may be affected by wind direction

[Please see comments above](#)

page 8, line 18: should say "...not a strong..." [done](#)

page 12, after line 16: should discuss potential of morning fog and/or NO₂

Please see comments above

page 13, line 1,2: boundary layer height inconsistent with modeling.

Please see comments above

page 13, line 28: why is Salar de Uyuni being discussed here?

Salar de Uyuni is the largest salt flat in the world and clearly enhanced BrO column densities have been detected by ground-based DOAS measurements in the past. It is briefly mentioned to make clear why other large salt lakes/marshes may not be easily observed by satellites using the DOAS technique due to spectral effects over high and bright surfaces.

We added this information to the manuscript.

page 14, line 11: clarify "supposed to"

Please see comments above

page 15, line 14: Wasn't OMAEROG also used, as well as either some level 1 OMI data or OMBRO (unclear).

We added the missing information to the Acknowledgement

page 22, caption says "adapted from Fund, W."? Typo?

Changed to "adapted from World Wildlife Fund:..."

Seasonal variation of tropospheric bromine monoxide over the Rann of Kutch salt marsh seen from space

C. Hörmann¹, H. Sihler^{1,2}, S. Beirle¹, M. J. M. Penning de Vries¹, U. Platt², and T. Wagner¹

¹Max-Planck-Institute for Chemistry (MPI-C), Mainz, Germany

²Institute for Environmental Physics, University of Heidelberg, Heidelberg, Germany

Correspondence to: C. Hörmann (c.hoermann@mpic.de)

Abstract. The Rann of Kutch (India/Pakistan) is one of the largest salt deserts in the world. Being a so-called 'seasonal salt marsh', it is regularly flooded during the Indian Summer Monsoon. We present 10 years of bromine monoxide (BrO) satellite observations by the Ozone Monitoring Instrument (OMI) over the Great and Little Rann of Kutch. OMI spectra were analysed using Differential Optical Absorption Spectroscopy (DOAS) and revealed recurring high BrO VCDs up to 1.4×10^{14} molec/cm² during April/May, but no significantly enhanced column densities during the monsoon season (June–September). In the following winter months, the BrO VCDs are again slightly enhanced while the salty surface dries up. We investigate a possible correlation of enhanced reactive bromine concentrations with different meteorological parameters and find a strong relationship between incident UV radiation and the total BrO abundance. In contrast, the second Global Ozone Monitoring Instrument (GOME-2) shows about four times lower BrO VCDs over the Rann of Kutch than found by OMI and no clear seasonal cycle is observed. One reason for this finding might be the earlier local overpass time of GOME-2 compared to OMI (around 9:30 **respectively** 13:30 LT), as the ambient conditions significantly differ for both satellite instruments at the time of the measurements. Further possible reasons are discussed and mainly attributed to instrumental issues. OMI additionally confirms the presence of enhanced BrO concentrations over the Dead Sea valley (Israel/Jordan), as suggested by **prior ground-based** observations. The measurements indicate that the Rann of Kutch salt marsh is **one** of the strongest natural point sources of reactive bromine compounds outside the polar **regions**.

1 Introduction

Reactive halogen species (RHS) are well known to play an important role in atmospheric chemistry of both the troposphere and stratosphere (e.g. Platt and Janssen, 1995; Saiz-Lopez and **von** Glasow, 2012, and references therein). For almost 30 years, **ground-based** observations in polar regions, at active volcanoes, within the mid-latitude marine boundary layer (MBL) and over salt lakes indicate the potential of these species to **influence** the oxidation capacity of the **troposphere significantly**, possibly on a global scale, via the catalysed depletion of ozone (O₃). After the so-called ozone depletion events (ODEs) were first observed in the 1980s by local measurements in the Arctic (Oltmans, 1981; Oltmans and Komhyr, 1986; Barrie et al., 1988), especially reactive bromine compounds were identified to be responsible for the ozone destruction. In particular, a strong anti-correlation **of** the ozone concentration with filterable bromine (**Barrie et al., 1988, 1989**) was found. In later studies, the

involvement of bromine chemistry was directly confirmed by additional measurements of bromine monoxide (BrO) using the Differential Optical Absorption Spectroscopy (DOAS) technique (Platt and Stutz, 2008), with BrO mixing ratios of up to 17 ppt (Hausmann and Platt, 1994). Subsequent observations showed even higher mixing ratios of up to 40 ppt (e.g. Avallone, 2003; Frieß, 2004; Hönninger et al., 2004; Pöhler et al., 2010; Peterson et al., 2015, and references therein). In the meantime, an overall picture of the total BrO horizontal distribution was obtained by observations from satellite instruments in the late 1990s (Wagner and Platt, 1998; Richter et al., 1998; Chance, 1998). A detailed analysis strongly indicated that the ODEs can be associated with huge tropospheric BrO 'clouds' of several thousands of km² extent, '(...) rather than by a disturbance of the stratospheric composition or a modification of the stratospheric AMF' (Wagner and Platt, 1998).

During the last three decades, BrO has also extensively been measured in the MBL by ground-based DOAS observations, but the observations revealed relatively low BrO mixing ratios of 1–10 ppt (e.g. Leser et al., 2003; Saiz-Lopez, 2004; Read et al., 2008; Martin et al., 2009). Volcanic BrO has not only been observed by a large number of ground-based DOAS observations at quiescent degassing volcanoes since the early 2000s (e.g. Bobrowski et al., 2003; Oppenheimer et al., 2006; Bobrowski and Platt, 2007; Boichu et al., 2011; Bobrowski and Giuffrida, 2012; Lübcke et al., 2014), but also during minor and major volcanic eruptions by satellite instruments (Theys et al., 2009a; Rix et al., 2012; Hörmann et al., 2013).

1.1 BrO observations over salt lakes

In contrast to BrO observations in other regions, reports about reactive halogen species observations over salt lakes were only infrequently published. Following the first ground-based DOAS observations of BrO over the Dead Sea with peak mixing ratios of 86 ppt by Hebestreit et al. (1999), later studies were able to confirm the results and found even higher mixing ratios of 220 ppt maximum (e.g. Matveev et al., 2001; Tas et al., 2005), representing the highest BrO mixing ratios observed in the atmosphere (outside volcanic plumes). The vertical distribution of BrO above the Dead Sea and the corresponding dynamics were more recently discussed in Holla et al. (2015). Much lower mixing ratios of up to 6 ppt were found over the Great Salt Lake (United States) by Stutz et al. (2002) as well as more than 20 ppt at Salar de Uyuni (Bolivia) by Hönninger et al. (2004). Further field campaigns were conducted by Holla (2012) in Namibia (Walfish Bay), Botswana (Sua Pan), South Russia (El'Ton and Baskuntschak), Mauretania (Sebkha N'Dramcha), South West Australia (Lake Stubbs, Lake Orr, Lake King, Lake Tay and Lake Chlorine) and Cape Verde (including artificial solar salt ponds at Santa Maria and the Pedra Lume caldera, which is filled with oceanic water). However, none of these measurements showed significantly enhanced BrO or iodine oxide (both less than 2 ppt or below the detection limit of the MAX-DOAS measurements). A model study by Tas et al. (2006) focusing on the Dead Sea emphasized the possibly important role of aerosols for the release of reactive bromine, while another study by Smoydzin and von Glasow (2009) suggested an additional direct bromine release from sea water. The autocatalytic reaction cycle that is associated with the rapid production of BrO (so-called 'bromine explosion', Platt and Lehrer, 1997) could recently be observed under laboratory conditions within a smog chamber (Buxmann et al., 2012). In the latter study, environmental conditions like salt composition, pH value, temperature and relative humidity (RH) were varied and a BrO build-up above a model salt pan could be studied in detail, indicating a strong dependency on RH - possibly controlled by the thickness of

resulting water microlayers on the salt crust. However, the detailed chemical mechanism still remain unclear as corresponding model calculations were not able to reproduce the findings.

1.2 The Rann of Kutch

The Rann of Kutch is a 'seasonal' salt marsh, stretching from the Indo-Pakistani border into the Kutch District of India's largest state, Gujarat (about 22.5-25.5°N, 67.5–72.5°E). With more than 30000 km² it is the largest salt desert in the world and additionally one of the hottest areas of India with summer temperatures around 50°C and winter temperatures decreasing below 0°C during night. The Rann (the name originates from the Hindi word for *desert*) can be subdivided into a large northern part ('Great Rann of Kutch') and the considerably smaller 'Little Rann of Kutch' (Figure 1), located at the south-eastern border of Gujarat. During India's summer monsoon (June/July - September/October), the flat desert of salty clay and mudflats (which lies, on average, 15 meters a.s.l.) is flooded by tidal water as well as freshwater from nearby rivers and standing water from extensive rainfall (Figure 2). Due to these rather extreme climatical conditions, the area is widely uninhabited. After the monsoon season, the accumulated shallow water layer evaporates, leaving large parts of the Rann covered by a snow white salt crust. Large industrial evaporation ponds are located near the coast of the Great and Little Rann of Kutch (indicated by red marked areas in Figure 2a, left) and used for the production of salt and the subsequent recovery of elemental bromine from sea bittern, i.e. mother liquor left after recovery of common sodium chloride from brine (Mehta et al., 2003). Especially all over the Little Rann, the salt is also harvested from hand-built salt evaporation ponds that are constructed by thousands of local families year after year (Pacha, 2013), after having been destroyed by the annually recurring monsoon flood (see also Figure 1–3 of the Supplementary Material). Atmospheric measurements by ground-based instruments have not been performed in the Rann of Kutch yet, probably due to the difficult climatic conditions. Satellite observations, however, provide the unique possibility to investigate the entire area remotely over a long time period.

2 Instruments

2.1 Ozone Monitoring Instrument

The Ozone Monitoring Instrument (OMI) is part of NASA's Earth Observation System (EOS) program and is carried by the Aura satellite, launched in July 2004 into a sun-synchronous polar orbit at 705 km altitude (Levelt et al., 2006). Aura crosses the equator at about 13:30 local time. The three channel UV/Vis push-broom spectrometer covers a wavelength range from 270–500 nm at a moderate spectral resolution of 0.42–0.63 nm. Featuring a two-dimensional CCD detector with a near nadir ground pixel size of 13×24 km² (up to 28×150 km² at the swath edge) and a large swath width of 2600 km, the measurements achieved daily global coverage until the first appearance of the so-called 'row anomaly' in June 2007. Today, global coverage is achieved after two days, as almost half of the OMI ground pixels are affected by the 'row anomaly' (KNMI, 2015). So far,

OMI has been successfully used to monitor enhanced BrO vertical column densities (VCDs) during polar spring, associated with the ODEs (e.g. Salawitch et al., 2010; Choi et al., 2012) and during volcanic eruptions (Theys et al., 2014).

2.2 Global Ozone Monitoring Experiment-2

The second generation of the Global Ozone Monitoring Experiment (GOME-2) is a series of three identical instruments that are part of the MetOp satellite program operated by the European Organisation for the Exploitation of Meteorological Satellites (EUMETSAT). The first GOME-2 instrument, GOME-2A, is carried by MetOp-A and was launched into a sun-synchronous polar orbit at 800 km altitude in October 2006 (Callies et al., 2000). The second instrument (GOME-2B, carried by MetOp-B) was launched in September 2012, GOME-2C will be carried by the MetOp-C satellite to be launched in 2018. MetOp-A crosses the equator at about 9:30 local time. In this study, only GOME-2A observations are analysed.

The GOME-2A instrument is a 4 channel UV/Vis grating spectrometer that observes the Earth's atmosphere in near-nadir viewing geometry. Originally, a scanning mirror provided a cross-track swath width of 1920 km (at observation angles up to 50° off-nadir) resulting in global coverage within 1.5 days (EUMETSAT, 2005; Munro et al., 2006). GOME-2A measures both the radiance of sunlight reflected by the Earth's atmosphere and the solar irradiance, covering the wavelength region of 240–790 nm at moderate spectral resolution of 0.2–0.4 nm. With a nadir pixel size of 40×80 km², GOME-2A observed 4 times smaller ground pixels than its predecessor GOME on ERS-2, but 10 times larger when compared to OMI ground pixels (see Section 2.1). After several test configurations in early 2013, the swath-width of GOME-2A was reduced to 960 km (nadir pixel size of 40×40 km²) to achieve daily global coverage via the so-called 'tandem operation' mode together with GOME-2B, which covers the remaining daily gaps. Like OMI, GOME-2(A) data have been successfully used to observe enhanced tropospheric BrO VCDs during polar spring (e.g. Begoin et al., 2010; Theys et al., 2011; Sihler et al., 2012) and during volcanic eruptions worldwide (Theys et al., 2009a; Hörmann et al., 2013).

3 BrO DOAS retrieval

The spectral data of both satellite instruments were analysed at MPI-C for BrO column densities by using the Differential Optical Absorption Spectroscopy (DOAS) technique (Platt and Stutz, 2008). The GOME-2 data was evaluated using the algorithm developed by Sihler et al. (2012). The OMI BrO retrieval follows the general settings of the GOME-2 retrieval: Level 1 data (online provided by the Goddard Earth Sciences Data & Information Services center, NASA) were analysed using a wavelength range from 336–360 nm, including 4 adjacent BrO absorption bands. In addition to the BrO cross section from Wilmouth et al. (1999), ozone cross sections at 223 and 243 K (Gür et al., 2005), O₄ (Greenblatt et al., 1997), NO₂ (Vandaele et al., 2002), OCIO (Bogumil et al., 2003) and SO₂ (Bogumil et al., 2003) were used. Furthermore, two Ring spectra (one calculated for a sun reference spectrum, the other one using the former scaled by λ^4), an inverse reference spectrum and a 5th order polynomial were included in the BrO retrieval.

OMI data affected by the 'row anomaly' (first appearing after June 25th, 2007) were excluded from the retrieval (KNMI, 2015). Due to differences in the measurement sensitivity of single CCD detector pixels, OMI BrO column density maps suffer from

cross-track striping, which is especially apparent for weak absorbers like BrO. To overcome the striping effect, mean **geomet-**
rical BrO VCDs (appropriate for an stratospheric absorber) calculated for each pixel row individually over a remote area over
the Pacific ($\pm 20^\circ\text{N}$, $105\text{--}175^\circ\text{W}$) were subtracted from all daily measurements. Since the contribution of stratospheric BrO
to the total column is hereby removed as well, the median BrO column across the track was re-added. Please note that the
5 BrO VCDs finally used in this study are corrected for the stratospheric contribution to the total column by a specifically local
separation (see Sect. 3.2).


The measured spectra are additionally affected by permanent and transient hot pixels, leading to increased noise at certain
wavelengths for individual CCD detector rows. Such erroneous measurements can be easily identified by abnormally large
fitting residuals at affected wavelength positions and again lead to strongly elevated BrO VCD stripes. Following the sugges-
10 tions by Chance (2007), intensities measured at pixels showing very strong residual discrepancies ($>4\sigma$) from an initial fit were
excluded for a final second fit. The vast majority of former suspiciously anomalous BrO slant column densities (SCDs) showed
realistic columns similar to nearby measurements after the correction.

3.1 Clouds

The observation of tropospheric trace gases is significantly affected by radiative transfer due to cloud coverage in several
15 ways. If the trace gas is located above a thick cloud layer, satellite measurements might show an increased sensitivity. On the
other hand, clouds may completely shield trace gases close to the surface. To minimize the influence of clouds, only OMI
measurements with an effective cloud fraction of less than 30% were considered. For this purpose two operational Level 2
OMI cloud products are provided by NASA:

1. OMCLDO2, for cloud detection using the $\text{O}_2\text{--O}_2$ absorption near 477 nm (e.g. Acarreta and de Haan, 2002; Vasilkov
20 et al., 2008)
2. OMCLDRR, using information of the so-called filling-in of solar Fraunhofer lines caused by rotational-Raman (RR)
scattering in the atmosphere (Ring effect) within the 346–354 nm spectral range (e.g. Joiner et al., 2002; Stammes et al.,
2008)

Although the OMCLDO2 algorithm is most commonly used, it turned out that the algorithm almost always mis-classifies
25 the bright surface of the salt marsh as cloud and is thereby unsuitable for the BrO analysis presented here. In contrast, the
OMCLDRR algorithm seems to better distinguish between the bright surface and clouds, probably because of an increased
contrast in the UV in comparison to the visible wavelength range that is used in the OMCLDO2 algorithm. It should, however,
be noted that a reanalysis of the data applying a lower cloud filter threshold of only 20% showed that the OMCLDRR algorithm
sometimes misinterprets the bright surface of the salt marsh as clouds as well. This is in particular the case during the first 3–4
30 months after the Rann is flooded (October/November–December/January). As the remaining water evaporates, a very clean and
bright surface remains as indicated by increased reflectivity; this effect can be seen in MODIS true color images as in Figure
2. In order to provide statistically relevant monthly averaged BrO VCDs, only grid pixels that were covered at least ten times
by the daily measurements were finally taken into account. It can, however, not be completely ruled out that some of the actual

cloud free measurements are sorted out using the cloud filter. 

For GOME-2, the only available cloud detection algorithms are the operational FRESCO (Koelemeijer and Stammes, 2001; Koelemeijer et al., 2002) and ROCINN (Loyola R., 2004; Rozanov et al., 2006) products, which both use wide parts of the oxygen A-band spectrum to determine the effective cloud fraction. Similar to the OMI OMCLDO2 algorithm, both FRESCO and
5 ROCINN fail to distinguish between the bright surface of the salt marsh and clouds. Therefore only a qualitative comparison of the unfiltered cloudy data will be presented in Section 4.5.

3.2 Local stratospheric background correction

Because all satellite measurements include the total atmospheric BrO column, the data have to be corrected for the stratospheric fraction to retrieve the tropospheric BrO column over the salt marsh area. The stratospheric BrO distribution **for lower latitude**
10 **regions (like the Rann of Kutch area)** varies little with latitude and even less with longitude (Theys et al., 2009b). Therefore, BrO VCDs determined assuming a geometrical airmass factor were corrected by subtracting the results of a two-dimensional spatial polynomial fit of 3rd degree n applied to the daily measurements as described in Hörmann et al. (2013):

$$V_{\text{trop},i}^* \approx V_{\text{tot},i}^* - \sum_{m,n=0}^3 V_{\text{strat},i}^* \times x_i^m \times y_i^n \quad (1)$$

where $V_{\text{strat},i}^*$ are the fitted stratospheric BrO VCDs at the centre coordinates x and y [°] of satellite pixel i within a large **area**
15 **around the Rann of Kutch (18–30°N, 62–78°E)**. To minimize the influence of possibly enhanced BrO VCDs over the salt marsh, the actual Rann area (22.5–25.5°N, **67.5–72.5°E**) was excluded from the polynomial fit of the stratospheric correction approach. The resulting corrected geometrical BrO VCDs (V_{trop}^*) were reconverted into 'tropospheric' SCDs (S_{trop}^*) by **multiplication**
with the geometrical AMF.

Please note that this rather simple approach can only be applied, because the stratospheric BrO gradients over the studied area
20 **are relatively small compared to the extent of the salt marsh. In general, an accurate quantification of tropospheric BrO VCDs (e.g. at high latitudes during arctic spring) needs a more sophisticated estimation of the stratospheric BrO contribution (e.g. Sihler et al., 2012).**

3.3 Radiative transfer

As the radiative transfer for a tropospheric absorber is not adequately represented by the geometrical approximation, the
25 'tropospheric' S_{trop}^* were multiplied with box air-mass factors (box-AMF) calculated by the Monte Carlo radiative transfer model (RTM) McArtim (Deutschmann et al., 2011) to retrieve final BrO VCDs. The simulations were conducted near the strongest BrO absorption band (338.5 nm) assuming cloud-free conditions. Two main model runs were performed for different homogeneous BrO layer profiles (0–400 m, 0–1 km and 0–2 km):

1. No additional aerosols (varying surface albedo of 0.10, 0.15 and 0.20)

2. Additional homogeneous aerosol layer at 0-1 km (single-scattering albedo (SSA): 0.9, asymmetry parameter (AP): 0.72 and varying aerosol optical depth (AOD) of 0.4, 0.7 and 1)

As baseline properties, a surface albedo of 0.15 (based on typical OMI reflectivity values at 331 nm; available via the NASA OMSO2 Level 2 OMI SO₂ product and briefly described in Carn et al., 2013), a homogeneous BrO layer at 0-1 km and an AOD of 0.7 were chosen. All baseline aerosol properties assumptions (AOD, SSA and AP) were based on monthly mean OMI observations at 342.5 nm (via the NASA OMAEROG Level 2 aerosol product, described in Torres et al., 2007). As the OMAEROG product often shows unrealistically high parameter values exclusively over the Rann area (e.g. monthly mean AODs of more than 4), the product seems to have some problems with the exceptionally bright surface of the salty desert. Additionally, the associated parameters seem to be affected by increased cloud coverage during the monsoon season. In order to estimate the actual aerosol parameters despite these problems, mean values for AOD, SSA and AP close to (but outside of) the Rann area were chosen.

It is important to note that the baseline scenario (assuming a homogeneous BrO layer between 0–1km) only represents a first guess of the true BrO profile, based on the assumption that BrO forms at the salt surface and is partly transported to higher altitudes. While the BrO profile can be expected to depend on the prevailing boundary layer height, the true profile over the Rann remains unknown (the BrO layer doesn't necessarily need to fill the complete boundary layer). An estimate of the uncertainties caused by the a priori assumptions is given in Section 4.2. For an adequate estimation of the true BrO profile, however, results from local ground-based MAX-DOAS measurements would be desirable in the future.

4 Results

The individual daily measurements of each month from October 2004 to December 2014 were gridded on a regular lat-lon grid with a spatial resolution of 0.1°, from which monthly mean BrO VCD maps were calculated. Figure 3 shows the monthly mean BrO VCDs (10-year-averages for 2004–2014) for baseline RT settings (see Section 3.3). It is clearly visible from the maps that the BrO VCDs slowly rise during the first months of each year and reach a maximum during April/May ($\approx 6 \times 10^{13}$ molec/cm²). In the second half of the year, the values are much lower. During the monsoon (June–September), the enhancement almost completely disappears. The low values during the monsoon are, however, at least partly caused by the shielding effect of remaining cloud cover over the observed area (as additionally indicated by enhanced background noise in the southeastern part of the shown region due to the reduced statistics). After the monsoon (October–December) the BrO VCDs remain at a low level, reaching magnitudes similar to those found at the beginning of the year. Although the individual years 2004–2014 partly show a less prominent seasonal variation of the absolute BrO VCDs over the salt marsh, the temporal evolution is similar for all analysed years (see Supplementary Material for all time series). The annual mean BrO VCD maxima were mostly found during April (2006–2009, 2011–2014) and twice in May (2005, 2010), with a 10-year-maximum of about 1.4×10^{14} molec/cm² in April 2009.

Regarding the Great Rann of Kutch, a closer look to the annual pattern indicates that the BrO VCDs typically first rise in the western part during March, before clearly enhanced VCDs can be seen over the whole area in April and mostly over the

middle/eastern part during May (Figure 3, March–May). It remains unclear if this behaviour originates in the different ambient conditions in different areas and months or if it is caused by transport due to a steady westerly wind (see Section 4.4 and Figure 7). A significant contribution of halogen emissions from the large artificial evaporation ponds that are used for salt/bromine mining is unlikely, as no trend can be seen from the measurements although the industrial facilities were massively expanded after 2009 (see Supplementary Material for MODIS observations of these industrial complexes).

The maximum BrO VCDs over the Little Rann of Kutch are generally lower compared to the Great Rann, with a maximum of 6.1×10^{13} molec/cm² in May 2010. Like for the Great Rann, the annual maximum BrO VCDs typically appear during April–May, but remain at a very low level close to the detection limit for all other months (Figure 3). Even during April/May, the maximum BrO VCDs over the Little Rann are about a factor of 3 lower than over the Great Rann.

A detailed comparison of the BrO VCDs with those from the operational NASA OMBRO product showed only small differences of typically 10%. For this purpose, the calculation of troposphere BrO VCDs was applied to the BrO slant columns from the OMBRO product in the very same way as for the SCDs retrieved at MPIC.

4.1 Variation of surface reflectivity and sensitivity

The strongly enhanced albedo of the salty crust is expected to have a significant effect on the sensitivity for near-surface BrO. This may lead to an apparently enhanced BrO VCDs over the Rann when compared to nearby areas featuring a lower albedo due to a potential enhanced tropospheric BrO background and the underestimation of the corresponding AMF. To investigate the possible influence of the bright surface on the spatial pattern of BrO VCDs, the reflectivity at 331 nm as seen by OMI (see Section 3.3) was used to calculate monthly averaged maps for the same data that were used for the BrO VCD maps (i.e. using a cloud filter CF<30%). Figure 4 shows the resulting mean reflectivity at 331 nm for 10-years-averaged months during 2004–2014. At first glance, especially the northern Great Rann of Kutch can be clearly identified for all months outside the monsoon season by the strongly increased reflectivity. During the monsoon (June–September) the shape of the salt marsh vanishes as the area is flooded and more and more (bright) clouds shield the Rann (despite the applied cloud selection criteria). The extensive cloud coverage generally leads to a widely enhanced mean reflectivity over the whole investigated area, especially the Indian mainland. After the monsoon, the mean reflectivity is typically even higher (20–23%) than during the first months of the year (15–20%), probably because the evaporating water leaves a clean, bright and salty crust. This effect can also be recognized in the corresponding MODIS true color images (compare Figure 2). A comparison of Figure 3 and 4 leads to the interesting finding that the reflectivity is smallest during months that typically show the highest BrO VCDs (April/May). The minimum reflectivity over the Great Rann appears for May 2005–2014 (as well as for most individual years; see Supplementary Material for all time series). Maximum BrO VCDs are found in April 2005–2014. Almost no BrO VCD enhancement can be observed after the monsoon months, whereas the reflectivity is highest. Generally, there is **not a** strong spatial correlation of the BrO VCDs to the mean reflectivity patterns. While there is only little variation in the regional reflectivity within the Rann area over different months, the spatial distribution of BrO VCDs changes and even seems to progress into the eastern part of the Great Rann from March–May (see Supplementary Material for a more detailed investigation of these effects). Although the enhanced albedo certainly contributes to the BrO enhancement observed over the Rann area (and is therefore considered for the AMF

calculations in Section 3.3, the BrO distribution cannot be generally explained by the bright surface as the distributions clearly differ.

In contrast to the Great Rann, the Little Rann cannot clearly be identified from averaged reflectivity maps as corresponding values stay close to surrounding areas ($\approx 7\text{--}10\%$), with the lowest values occurring during May 2005–2014, when enhanced

5 BrO VCDs clearly show up.

4.2 Estimation of total BrO mass and mixing ratio

To estimate the total amount of BrO for each month, the BrO VCDs within the Rann area ($22.5\text{--}25.5^\circ\text{N}$, $67.5\text{--}72.5^\circ\text{E}$) were summed up and converted into total masses ($M_{\text{BrO}}=95.903\text{ g/mol}$) by assuming the afore-mentioned baseline properties (i.e. a BrO layer thickness of 1 km; see Section 3.3). Figure 5 shows the resulting BrO mass over the Rann in the time period
10 between October 2004 and December 2014 (blue areas) next to the BrO mass determined from a neighbouring reference area of the same size to the west of the Rann region (red line). For the sake of clarity, all measurements that fall within the monsoon season (June–September) are indicated in green. Corresponding reflectivity values are shown by the blue dotted line.

The largest BrO amount can be regularly observed in April/May, ranging from 2100t in May 2007 up to 4700t in May 2010. Taking into account all OMI measurements, the mean BrO mass during spring (March–May) is calculated to be $(2700\pm 917)\text{t}$,
15 where the uncertainty represents the corresponding standard deviation σ . In contrast, the mean mass over the reference area was found to be about a factor of 13 lower $(212\pm 105)\text{t}$. The deviation from zero can probably be attributed to the imperfect polynomial correction for the stratospheric BrO background. During the monsoon season (June–September) the BrO mass declines over the Rann and remains at a comparatively low level of $(1066\pm 753)\text{t}$, often followed by a local maximum directly after the monsoon (October) before another minor drop leads to an annual minimum around December. While the mean

20 BrO masses over the Rann during the monsoon are still about 3x larger than over the corresponding reference area for most years $(279\pm 138)\text{t}$, they are associated with a high uncertainty due to the influence of cloud coverage and associated small number of measurements. In this context it should be mentioned that the reference area is generally less affected by (convective/orographic) clouds as large parts are located over the Arabian Sea. During wintertime (November–February), the mean BrO masses remain at the same low level $(1067\pm 560)\text{t}$ for the area over the Rann, $(187\pm 131)\text{t}$ over the reference area), however, the uncertainties are now much smaller as the Rann region is only sporadically affected by clouds.

Assuming a standard atmosphere and the baseline properties for the BrO layer (0–1 km), mixing ratios of 20–66 ppt maximum can be roughly estimated from the maximum BrO VCDs during March–May 2005–2014 (mean mixing ratio: $35\pm 10\text{ ppt}$). In reality, however, the mixing ratios remain highly uncertain as the true atmospheric properties (in particular the BrO vertical profile and the aerosol amount) are unknown. To point out the strong influence of all presumed parameters for the mixing ratio
30 estimation (i.e. the AMF calculation and the assumption of the BrO layer height), Table 1 shows the results for a variation of all key parameters in comparison to the baseline scenario. While varying aerosol parameters or even the general presence of aerosols (i.e. $\text{AOD}=0$) only lead to small changes (-8 to 6%) of the estimated BrO mixing ratio, a variation of the surface albedo (-14 to 20%) and especially the BrO layer thickness (-23 to 34%) has a rather strong effect on the corresponding mixing ratios. Overall, the final uncertainties can be estimated to be about -33 to 73% .

4.3 Correlation with meteorological parameters

The influence of meteorological parameters on the 'bromine explosion' reaction cycle is still largely unclear and remains a subject of intensive discussion within the scientific community. Several studies (e.g. Theys et al., 2009b; Choi et al., 2012; Sihler et al., 2012) discussed the influence of a high boundary layer height on the BrO satellite retrieval over Arctic regions. Recently,

5 Lieb-Lappen and Obbard (2015) analysed the role of blowing snow in the activation of bromine over first-year Antarctic sea ice. However, regarding the formation of BrO over salt lakes, the influence of environmental conditions like temperature, relative humidity or pH value were almost exclusively investigated by Buxmann et al. (2012). By using an artificial salt pan within a smog chamber, it was found that the corresponding BrO mixing ratios were almost one magnitude higher at a relative humidity of 60% when compared to experiments at 37% or 2%. This is probably caused by quasi-liquid water layers on the salty crust
10 that seem to support the activation of reactive bromine.

To investigate possible dependencies of the observed total BrO mass over the Rann of Kutch on humidity and other parameters, data from the European Centre for Medium-Range Weather Forecasts (ECMWF) for the whole investigated time period and within a $1^\circ \times 1^\circ$ area located over the central part of the Great Rann ($23.5\text{--}24.5^\circ$ N, $69\text{--}70^\circ$ E) were used to calculate monthly averaged values for different meteorological parameters around the time of the OMI overpass (9 UTC). Figure 6 shows the annual variation of the BrO mass together with total precipitation (P), cloud coverage (CC), relative humidity (RH), temperature (T), boundary layer height (BLH) and UV radiation at the surface (UV_{rad}). At first glance, the parameters can be divided into
15 two groups by their seasonal behaviour (indicated by different colours for left and right column in Figure 6a–f). While P, CC and RH are closely related to the Indian monsoon, T, BLH and UV_{rad} are closely related to each other via their dependence on solar irradiation. The latter three parameters correlate very well with the total BrO mass during the first half-year, before a second maximum shows up after the end of the monsoon. Focusing on the first half-year (i.e. the gradual increase of observed BrO VCDs starting in January until the beginning of the monsoon season in June), a linear fit applied to the BrO mass leads to high correlation coefficients for T ($r^2=0.87$), BLH ($r^2=0.93$) and UV_{rad} ($r^2=0.85$). In contrast, the other parameters show no correlation to the BrO mass as indicated by r^2 values of 0.03 (P), 0.05 (CC) and 0.03 (RH).
20

To further investigate whether a combination of these quantities can be used to model the annual BrO variation over the salt
25 marsh, a systematic multilinear regression analysis was conducted. Starting from a single parameter up to a combination of all six (P, CC, RH, T, BLH and UV_{rad}), a simple linear function was determined to describe the observed BrO cycle. The resulting r^2 value for each linear fit of the total BrO mass and individual multivariable function was finally used to indicate the goodness of fit. Figure 6g depicts the model results for all functions featuring the highest r^2 value for a given number of parameters. Table 2 additionally lists the corresponding fit results and r^2 values. For a single variable, a linear function (LF) depending on
30 the incident UV radiation already describes the annual BrO variations fairly well ($r^2=0.70$, purple dashed line in Fig. 6g). As the UV radiation remains a permanent component of all resulting functions independent of the total number of fitted variables, the photochemical aspect of the 'bromine explosion' is emphasized. Surface temperature appears to have a nearly negligible influence and is only included for the fit function featuring all six parameters ($r^2=0.97$, LF6, red dashed line in Fig. 6g), showing almost identical results when compared to LF5 (including all parameters but temperature). Especially precipitation and relative

humidity are clearly needed to fit the low level BrO variations during the monsoon and wintertime as can be seen by LF2/3 (light blue and orange dashed line in Fig. 6g, $r^2=0.83/0.91$). Taking into account four parameters (UV_{rad} , CC, RH and BLH) already leads to a linear function (LF4, black dashed line in Fig. 6g) that is well capable of describing all main features of the mean annual BrO observations ($r^2=0.95$). Interestingly (but self-evident), the features that were contributed by accounting for the precipitation appear to be widely included in the CC parameter for LF4, as both parameters are closely related to each other (the second highest r^2 value for LF3, 0.86, was achieved by using CC instead of P).

The seasonal cycle of BrO formation over the Rann of Kutch can be described reasonably well as a linear function of meteorological parameters for the 10 years averaged data on a monthly basis. It should, however, be noted that this simple approach fails to adequately reproduce the seasonal cycle when monthly averages from individual years are considered. In particular, the less pronounced BrO maxima in 2007/2008/2011/2012 are clearly underestimated and also the highly variable winter months are not very well captured by the linear functions. It has to be kept in mind that a linear model assumption of independent variables constitutes a rather simplistic approach to describe the satellite observations and can therefore only be used to get a rough idea about the general circumstances that are needed for the extensive formation of BrO over the salt marsh.

4.4 Seasonal wind pattern

Other possible parameters that might (at least indirectly) influence the 'bromine explosion' mechanism and the observed BrO spatial pattern are wind speed and main direction. Figure 7 and 8 (upper panels) show the 10-years-averaged monthly BrO VCDs over the Rann of Kutch along with the corresponding mean wind pattern that were calculated using daily ECMWF data (9 UTC). The lower panels in Figure 7 and 8 additionally illustrate the wind speed and the frequency of different wind directions. Starting with slow northeastern winds in January (≈ 2 m/s), the wind blows into eastern direction during months exhibiting strongly enhanced BrO VCDs (March–May). Towards the monsoon season, the winds get significantly stronger (up to 4 m/s in May) and reach their maximum strength in July with more than 7 m/s during 90% of all days, consistently coming from WSW. During these months, the strong wind speed supports the flooding of the Rann area by tidal water from the Arabian Sea. After the monsoon, the wind speed drops rapidly (1–2 m/s) and the wind turns towards east again. The following winter time is dominated by calm winds from the Northeast.

It is interesting to realize that the distinct seasonal wind patterns over the Rann of Kutch can be linked to different phases of the observed BrO occurrence. Apart from the close to zero BrO VCDs during the monsoon months that are dominated by strong winds from the southwest, the maximum BrO VCDs in March–May are accompanied by slow westerly winds, while the low BrO VCDs during wintertime are influenced by slow winds from the northeast. As mentioned above, the low BrO VCDs during the monsoon are at least partly caused by cloud shielding. Outside the monsoon season, the different wind patterns lead to differences in the effective time that an air mass stays in close contact to the salty crust of the Rann. Because the Great Rann of Kutch expands about 250 km from East to West (but only about 70 km from North to South), single air packages ideally may have remained about four times longer over the Great Rann for westerly wind conditions in April than during December, which is dominated by wind coming from the north. Aerosol particles that are needed for the 'bromine explosion' mechanism might therefore have an increased probability to be swirled up from the salty surface crust in significant amounts

during springtime. An examination of the actual aerosol appearance over the Rann remains, however, difficult, as available satellite aerosol products are strongly influenced by the bright surface of the salt marsh (see also Section 3.3).

For the Little Rann of Kutch, the wind direction has a much lower influence on the residence time of the air over the salt marsh, as this part of the salt marsh is much smaller and only slightly stretched in east-western direction ($\approx 50 \times 80$ km).

5 4.5 Comparison of OMI results with GOME-2 observations

The GOME-2 instrument overpasses the Rann of Kutch at about 9:30 local time (and therefore 4 hours before OMI). To investigate the diurnal evolution of BrO VCDs over the Rann area, 5 years of GOME-2 data (2007–2011) were evaluated for BrO in a similar way as for OMI (see Section 3 for details). As mentioned in Section 3.1, no cloud filter could be applied without losing a significant number of probably cloud free GOME-2 observations because the operational cloud products mistakes the bright surface for clouds. Therefore, only a qualitative seasonal intercomparison of the data will be presented in the following: No cloud filter is used and consequently, a *geometrical* AMF is used to calculate BrO VCDs (i.e. the data are only corrected for the viewing geometry; explicit radiative transfer calculations are not involved). Although geometrical AMFs are not well suited to quantitatively determine the BrO VCD over the Rann, they still can be used to visualize BrO abundances exceeding the comparably smooth stratospheric background. Please note that the geometrical AMF is this time also applied to OMI data to guarantee the consistency of both data sets. Because fully cloudy cases are not filtered out, low BrO VCDs are not only due to small near-surface BrO concentrations, but also to cloud shielding (possibly even outside of the monsoon season). However, it should be noted that most days outside the monsoon months (June–September) are only effected by low cloud fractions according to MODIS and ECMWF data. In addition, no differences in cloud cover were found that could be attributed to the different overflight time of the instruments throughout the year.

As it can be seen from Figure 9 (lower panel), the seasonal mean BrO VCD maps only indicate a very low enhancement over the salt marsh, which is close to background noise level. Please note that the GOME-2 BrO VCDs are presented using the same colorbar as the corresponding OMI results (Figure 9, upper panel) to emphasize the low levels of the GOME-2 BrO VCDs. During the monsoon season (here July–September, Figure 9, lowermost left panel), neither satellite instrument detects a clear enhancement, as massive cloud coverage shields the salt marsh area, but whereas OMI data clearly show a seasonal cycle with a pronounced maximum in April–June, no obvious seasonal variation can be seen in the GOME-2 data. One explanation for the very small BrO VCDs measured by GOME-2 (compared to OMI) may be differences in chemistry due to different ambient conditions at the early overpass time of GOME-2 (see below). Furthermore, the weak BrO VCD enhancement in the GOME-2 data could at least be partly caused by radiative transfer effects due to the increased surface albedo of the salt marsh. However, as the surface albedo shows a typical seasonal variation in contrast to the GOME-2 BrO VCDs (see Figure 4), this effects seems to be rather small. While radiative transfer simulations suggest a possible overestimation of the BrO VCDs by a factor of 1.5 (50%) due to an inadequate consideration of the bright surface (Section 3.3), this effect can be neglected for OMI, where peak BrO VCDs over the Rann are up to a factor of 16 larger than for areas outside the Rann at low surface albedo.

In principle, there are several instrumental and chemical reasons why the BrO VCDs over the Rann of Kutch derived from

GOME-2 are lower than those from OMI:

1. The spatial resolution of the GOME-2 instrument is $40 \times 80 \text{ km}^2$, while the near nadir ground pixel size of OMI is $13 \times 24 \text{ km}^2$. GOME-2 spectra are therefore generally expected to be less sensitive to localised emission sources, as larger ground pixels include a larger fraction of sunlight from areas outside the investigated object (the typical extent of the salt marsh area showing clearly enhanced BrO VCDs is less than that of a GOME-2 ground pixel).
2. GOME-2 is known to suffer from instrumental degradation (especially in the UV wavelength region) starting in 2008/2009 (Dikty and Richter, 2012). A significant increase in the scatter of retrieved VCDs has been observed, particularly for BrO. This, in addition to the generally low signal-to-noise-ratio of GOME-2 in the UV compared to OMI (Fioletov et al., 2013), has led to a lower sensitivity of the instrument to small BrO concentrations.
3. One of the main chemical reasons for much lower BrO VCDs using GOME-2 might be that the measurements take place about 4 hours earlier when compared to OMI observations ($\approx 9:30$ vs. $13:30$ LT). At the time of the morning overpass, the 'bromine explosion' mechanism has presumably not progressed very far, as solar irradiance is approximately 50% less than during OMI's afternoon overpass (according to ECMWF data) and the process is photolytically driven. Furthermore, O_3 is needed for the rapid build-up of BrO, which might be more easily available during the morning on the one hand, but may lead to differences in the spatial BrO distribution patterns for GOME-2 when compared to OMI. Observations at the Dead Sea (Israel) have shown that the largest BrO VCDs can be expected close to noontime, if enhanced NO_x levels are generally present due to anthropogenic pollution (Holla et al., 2015). In contrast to the Dead Sea area, however, neither OMI nor GOME-2 observations show significantly enhanced NO_2 VCDs over the Rann of Kutch area, but only in the vicinity of the cities Karachi ($\approx 300\text{--}400\text{km}$ away) and Ahmadabad ($\approx 200\text{--}300\text{km}$ away). A possible influence of NO_2 at the Rann of Kutch is therefore assumed to be much less important than over the Dead Sea.
4. The boundary layer height during the GOME-2 overflight in April/May is significantly lower ($\approx 2\text{km}$) than for the OMI measurements ($\approx 3\text{km}$). As the BLH increases towards noon, BrO originating from the ground might be transported to higher altitudes where it could be more easily detected by the OMI as the instrument's sensitivity generally increases for elevated layers. Additionally, the increasing BLH might lead to an increased mixing-in of tropospheric O_3 from higher altitudes and thereby lead to further formation of BrO. It is important to emphasize that the data shown in Figure 9 were only calculated by application of a geometrical AMF and therefore possible differences for the BLH and BrO profile are not taken into account. However, in the case of a homogeneous BrO layer filling in the complete boundary layer, corresponding radiative transfer effects would only result in about 15% differences for the resulting BrO VCDs and can therefore not explain the GOME-2 BrO VCDs close to background level.
5. Other meteorological parameters (like relative humidity) are expected to influence the efficiency of the 'bromine explosion' (Buxmann et al., 2012). While surface temperature (and associated parameters like e.g. boundary layer height) are

lower during the GOME-2 overflight, relative humidity is about 30% higher. However, the detailed role of meteorological conditions on the 'bromine explosion' mechanism remain unclear (see Section 4.3).

Although all of these effects probably contribute to the observed differences between OMI and GOME-2 observations, the reasons for these discrepancies are still a matter of further research. The best way to analyze the influence of ambient conditions on BrO formation would be an extensive ground-based measurement campaign. Such local observations would provide high temporal resolution data of meteorological parameters like wind speed and direction, relative humidity, boundary layer height, clouds (and morning fog) as well as a possible influence of anthropogenic pollution.

4.6 The Dead Sea (Israel/Jordan)

OMI data were additionally analysed over another salt lake, the Dead Sea, but the results will only be shortly discussed in the following. A more detailed analysis of the data (or for further locations) exceeds the scope of this paper.

As already mentioned in Section 1.1, BrO over the Dead Sea has been frequently observed by ground-based DOAS measurements during recent years. While the results of Hebestreit et al. (1999) suggested that the salt pans over the southern part of the Dead Sea are the main source of the observed BrO, Matveev et al. (2001) and Tas et al. (2005) concluded that BrO is produced over all parts of the sea, although the frequency and intensity of BrO production seemed to be more intense over the southern basin. Figure 10 shows the mean BrO VCDs for summer months with relatively low cloud coverage (April–October) for the complete data set from 2005–2014, including an additional cloud filter of <30%. As it can be seen from the map, the mean BrO VCDs are clearly enhanced over the southern part of the Dead Sea, while only weakly enhanced VCDs can be identified over the northern part. The results seem to confirm the ground-based findings, although the maximum BrO VCDs are shifted towards the southwestern inland, probably because of northeasterly winds that predominate in this area (Matveev et al., 2001).

It is interesting to note that the BrO VCDs found over the Dead Sea are generally much lower than those observed over the Rann of Kutch, although the above-mentioned ground-based measurements showed the highest BrO mixing ratios so far observed at a salt lake (up to 220ppt). This finding indicates that the Rann of Kutch is likely one of the strongest natural point sources of reactive bromine compounds outside the polar regions. This argument is further strengthened by the fact that the Rann is the only salt lake/marsh, where a clear enhancement of the BrO column can be easily seen during several months from satellite measurements (even without correcting for the stratospheric background or excluding clouded data). However, BrO from other salt lakes (particularly smaller ones, like the Dead Sea) may generally not be identified as easily from the OMI data for several reasons. Besides lower BrO concentrations, DOAS satellite observations of optically weak absorbers like BrO are known to suffer from erroneous evaluation results caused by imperfect correction of the Ring effect (Wagner et al., 2009). This effect appears more prominent if the measured scene contains high elevation and bright surfaces like snow-covered mountain ranges in combination with strong cloud coverage during the year (e.g. as it is the case for the largest salt flat in the world, Salar de Uyuni in the Andes, Chile). The OMI BrO analysis of individual months over the Dead Sea reveals that the whole Middle East region is indeed more regularly affected by clouded scenes when compared to the Kutch area. Resulting monthly mean maps were hence significantly affected by low statistics. Furthermore, the analysis is complicated by the mountainous areas

along the Jordan and Hula Valley and the associated influence on the correction of the Ring effect. In this context it should be noted that significantly enhanced BrO VCDs were frequently observed north of the Dead Sea Valley and close to Tripoli, Libya (not shown). As there is no obvious source for reactive bromine species to the authors' knowledge, it remains unclear if these findings are caused by residual structures in the DOAS evaluation or actually caused by unknown bromine sources.

5 5 Conclusions

Satellite measurements have been used to monitor the seasonal cycle of BrO formation over the Rann of Kutch seasonal salt marsh. In particular, we presented the first space-based measurements of BrO originating from a salt marsh/salt lake, emphasizing the capability of satellite instruments to monitor remote and hardly accessible areas for long-term measurements. Up to now, no ground-based atmospheric measurements have been conducted at the Rann of Kutch to the authors' knowledge, despite (or precisely because of) the unique environmental conditions prevailing on-site. The results indicate that the Rann of Kutch salt marsh is probably one of the strongest natural point sources of reactive bromine compounds outside the polar regions and is therefore supposed to have a significant impact on local and regional ozone chemistry.

The OMI measurements reveal a typical annual BrO formation cycle over the Rann, with maximum BrO VCDs appearing during March–May, coinciding with the strongest UV irradiation at the surface. These findings confirm that BrO is not directly emitted from the surface, but driven by photochemistry, which involves the release of BrO precursors like molecular bromine (Br_2) as a part of the autocatalytical 'bromine explosion'. During the monsoon (June–September), the whole Rann of Kutch area is flooded, and a massive decrease of the BrO VCDs is observed. This effect is, however, partially caused by increased cloud cover, as shielding of the surface strongly affects satellite measurements of trace gases close to the ground. Only slightly enhanced BrO VCDs show up in wintertime (November–February). No clear influence of the Rann's surface albedo can be seen from OMI UV reflectivity measurements. While enhanced BrO VCDs may appear due to an unconsidered increase of the surface albedo, the Rann's surface appears relatively dark during the time of the maximum BrO VCDs (probably because of first moistening towards the monsoon season) and BrO can be hardly detected during the winter months, when the surface appears brightest.

A first attempt to describe the annual BrO cycle based on a simple linear parametrisation of different meteorological quantities indicates that, in addition to UV irradiation, the variation of the boundary layer height is an essential parameter needed to describe the annual BrO peak, which can be at least partly explained by the higher sensitivity of the satellite for elevated layers. For an adequate description of the near-surface BrO variations, relative humidity and precipitation also play an important role. The seasonal wind conditions can be additionally linked to the observed seasonal variation of the BrO VCDs: The maximum VCDs in March–May are accompanied by westerly winds, which may lead to an increased swirling up of aerosol particles due to the east-west expansion of the Rann and the thereby increased residence time of air masses over the salt crust. In contrast, low VCDs during wintertime are affected by slow winds from the northeast.


Corresponding GOME-2 measurements during the morning (4 hours earlier than OMI) show about 4 times lower BrO VCDs and no clear seasonal cycle, aside from minimum column densities during the strongly cloud affected monsoon months. **AI-**

though instrumental reasons may contribute to these findings, the results indicate the fundamental influence of ambient meteorological conditions at the time of the satellite overflight (e.g. the UV radiation at the surface is about 50% lower), and that the 'bromine explosion' still needs to evolve during the morning hours in order to allow BrO concentrations to build up to values that may be detected from space.


- 5 Additional OMI measurements of enhanced BrO VCDs over the Dead Sea demonstrate the potential of satellite instruments for the global observation of reactive halogen species over salt lakes. By the improved temporal and in particular spatial resolution of upcoming satellite instruments like the TROPospheric Monitoring Instrument (TROPOMI, Veefkind et al., 2012, launch expected for mid 2016), the number of daily salt lake observations will further increase. Furthermore, satellite instruments on geostationary orbits featuring several measurements per day over the same location like Sentinel-4 (Ingmann et al., 2012, expected for 2019) will allow to investigate the diurnal evolution of the 'bromine explosion' in more detail (not only over salt lakes). However, as it was stated by Saiz-Lopez and von Glasow (2012), "A regional or global assessment of the relevance of halogen chemistry over salt lakes and saline soils is so far missing". The significantly enhanced BrO VCDs over the Rann of Kutch in combination with the unique local conditions on the other hand strongly suggest to undertake a ground-based measurement field campaign in that area to better constrain the general release mechanisms of reactive bromine compounds
- 15 from salt marshes and lakes as well as their impact on atmospheric chemistry.

Acknowledgements. We would like to thank the agencies providing the satellite data: OMI Level 1 data as well as the Level 2 products OMSO2 (including reflectivity at 331nm), OMBRO, OMCLDO2, OMCLDRR, OMAEROG products and MODIS AQUA/TERRA true color and channel 7-2-1 images are archived and distributed from the Goddard Earth Sciences Data & Information Services center (NASA). We acknowledge EUMETSAT for providing GOME-2A Level 1 data and ECMWF for providing meteorological parameters over India/Pakistan.

References

- Acarreta, J. R. and de Haan, J. F.: Cloud Pressure Algorithm Based on O₂–O₂ Absorption, Chapter 2 in: OMI Algorithm Theoretical Basis Document, Volume III - Clouds, Aerosols, and Surface UV Irradiance, Version 2.0, pp. P. 17–30, available at: <http://eospsso.gsfc.nasa.gov/sites/default/files/atbd/ATBD-OMI-03.pdf>; last access on 28 January 2016, 2002.
- 5 Avallone, L. M.: In situ measurements of bromine oxide at two high-latitude boundary layer sites: Implications of variability, *Journal of Geophysical Research*, 108, doi:10.1029/2002JD002843, 2003.
- Barrie, L. A., Bottenheim, J. W., Schnell, R. C., Crutzen, P. J., and Rasmussen, R. A.: Ozone destruction and photochemical reactions at polar sunrise in the lower Arctic atmosphere, *Nature*, 334, 138–141, doi:10.1038/334138a0, 1988.
- Barrie, L. A., den Hartog, G., Bottenheim, J. W., and Landsberger, S.: Anthropogenic aerosols and gases in the lower troposphere at Alert, Canada, in April 1986, *Journal of Atmospheric Chemistry*, 9, 101–127, doi:10.1007/BF00052827, 1989.
- 10 Begoin, M., Richter, A., Weber, M., Kaleschke, L., Tian-Kunze, X., Stohl, A., Theys, N., and Burrows, J. P.: Satellite observations of long range transport of a large BrO plume in the Arctic, *Atmos. Chem. Phys.*, 10, 6515–6526, doi:10.5194/acp-10-6515-2010, 2010.
- Bobrowski, N. and Giuffrida, G.: Bromine monoxide / sulphur dioxide ratios in relation to volcanological observations at Mt. Etna 2006–2009, *Solid Earth*, 3, 433–445, doi:10.5194/se-3-433-2012, 2012.
- 15 Bobrowski, N. and Platt, U.: SO₂/BrO ratios studied in five volcanic plumes, *J. Volcanol. Geoth. Res.*, 166, 147–160, doi:10.1016/j.jvolgeores.2007.07.003, 2007.
- Bobrowski, N., Hönninger, G., Galle, B., and Platt, U.: Detection of bromine monoxide in a volcanic plume, *Nature*, 423, 273–276, doi:10.1038/nature01625, 2003.
- Bogumil, K., Orphal, J., Homann, T., Voigt, S., Spietz, P., Fleischmann, O., Vogel, A., Hartmann, M., Kromminga, H., Bovensmann, H., Frerick, J., and Burrows, J.: Measurements of molecular absorption spectra with the SCIAMACHY pre-flight model: instrument characterization and reference data for atmospheric remote-sensing in the 230–2380 nm region, *Journal of Photochemistry and Photobiology A: Chemistry*, 157, 167–184, doi:doi: 10.1016/S1010-6030(03)00062-5, 2003.
- 20 Boichu, M., Oppenheimer, C., Roberts, T. J., Tsanev, V., and Kyle, P. R.: On bromine, nitrogen oxides and ozone depletion in the tropospheric plume of Erebus volcano (Antarctica), *Atmos. Environ.*, 45, 3856–3866, doi:10.1016/j.atmosenv.2011.03.027, 2011.
- 25 Buxmann, J., Balzer, N., Bleicher, S., Platt, U., and Zetzsch, C.: Observations of bromine explosions in smog chamber experiments above a model salt pan, *International Journal of Chemical Kinetics*, 44, 312–326, doi:10.1002/kin.20714, 2012.
- Callies, J., Corpaccioli, E., Eisinger, M., Hahne, A., and Lefevre, A.: GOME-2 - MetOp's Second Generation Sensor for Operational ozone Monitoring, *ESA Bulletin*, 102, 2000.
- Carn, S. A., Krotkov, N. A., Yang, K., and Krueger, A. J.: Measuring global volcanic degassing with the Ozone Monitoring Instrument (OMI), Geological Society, London, Special Publications, 380, SP380.12, doi:10.1144/SP380.12, 2013.
- 30 Chance, K.: Analysis of BrO measurements from the Global Ozone Monitoring Experiment, *Geophysical Research Letters*, 25, 3335–3338, doi:10.1029/98GL52359, 1998.
- Chance, K.: OMBRO–OMHCHO–OMOCLO De-Striping README FILE, http://ozoneaq.gsfc.nasa.gov/media/docs/OMSAO_DeStriping_README.pdf, last access on 28 January 2016, 2007.
- 35 Choi, S., Wang, Y., Salawitch, R. J., Canty, T., Joiner, J., Zeng, T., Kurosu, T. P., Chance, K., Richter, A., Huey, L. G., Liao, J., Neuman, J. A., Nowak, J. B., Dibb, J. E., Weinheimer, A. J., Diskin, G., Ryerson, T. B., da Silva, A., Curry, J., Kinnison, D., Tilmes, S., and Levelt, P. F.: 

- Analysis of satellite-derived Arctic tropospheric BrO columns in conjunction with aircraft measurements during ARCTAS and ARCPAC, *Atmos. Chem. Phys.*, 12, 1255–1285, doi:10.5194/acp-12-1255-2012, <http://www.atmos-chem-phys.net/12/1255/2012/>, 2012.
- Deutschmann, T., Beirle, S., Frieß, U., Grzegorski, M., Kern, C., Kritten, L., Platt, U., Prados-Román, C., Pukite, J., Wagner, T., Werner, B., and Pfeilsticker, K.: The Monte Carlo atmospheric radiative transfer model McArtim: Introduction and validation of Jacobians and 3D features, *J. Quant. Spectrosc. Ra.*, 112, 1119–1137, doi:10.1016/j.jqsrt.2010.12.009, 2011.
- Dikty, S. and Richter, A.: GOME-2 on MetOp-A Support for Analysis of GOME-2 In-Orbit Degradation and Impacts on Level 2 Data Products, final report, October 2011, http://www.iup.uni-bremen.de/doas/reports/Final_Report_Level-2_Data_GOME-2_Degradation.pdf, last access on 28 January 2016, 2012.
- EUMETSAT: GOME-2 Product Guide, available at: <http://www.eumetsat.int/website/home/Satellites/CurrentSatellites/Metop/MetopDesign/GOME2/index.html>; last access on 28 January 2016, 2005.
- Fioletov, V. E., McLinden, C. A., Krotkov, N., Yang, K., Loyola, D. G., Valks, P., Theys, N., Van Roozendaal, M., Nowlan, C. R., Chance, K., Liu, X., Lee, C., and Martin, R. V.: Application of OMI, SCIAMACHY, and GOME-2 satellite SO₂ retrievals for detection of large emission sources, *Journal of Geophysical Research: Atmospheres*, 118, 11,399–11,418, doi:10.1002/jgrd.50826, 2013.
- Frieß, U.: Dynamics and chemistry of tropospheric bromine explosion events in the Antarctic coastal region, *Journal of Geophysical Research*, 109, doi:10.1029/2003JD004133, 2004.
- Greenblatt, G. D., Orlando, J. J., Burkholder, J. B., and Ravishankara, A. R.: Absorption Measurements of Oxygen Between 330 and 1140 nm, *Journal of Geophysical Research*, 95, PP. 18,577–18,582, doi:10.1029/JD095iD11p18577, 1997.
- Gür, B., Spietz, P., Orphal, J., and Burrows, J. P.: Absorption Spectra Measurements with the GOME-2 FMs using the IUP/IFE-UBs Calibration Apparatus for Trace Gas Absorption Spectroscopy VATGAS, Final Report, University of Bremen, October 2005, 2005.
- Hausmann, M. and Platt, U.: Spectroscopic measurement of bromine oxide and ozone in the high Arctic during Polar Sunrise Experiment 1992, *J. Geophys. Res.*, 99, 25 399–25 413, doi:10.1029/94JD01314, 1994.
- Hebestreit, K., Stutz, J., Rosen, D., Matveiv, V., Peleg, M., Luria, M., and Platt, U.: DOAS Measurements of Tropospheric Bromine Oxide in Mid-Latitudes, *Science*, 283, 55–57, doi:10.1126/science.283.5398.55, 1999.
- Hönninger, G., Leser, H., Sebastián, O., and Platt, U.: Ground-based measurements of halogen oxides at the Hudson Bay by active longpath DOAS and passive MAX-DOAS, *Geophysical Research Letters*, 31, doi:10.1029/2003GL018982, 2004.
- Holla, R.: Reactive Halogen Species above Salt Lakes and Salt Pans, Ph.D. thesis, University of Heidelberg, available online at http://archiv.ub.uni-heidelberg.de/volltextserver/14636/1/Dissertation_Holla_Robert.pdf, 2012.
- Holla, R., Schmitt, S., Frieß, U., Pöhler, D., Zingler, J., Corsmeier, U., and Platt, U.: Vertical distribution of BrO in the boundary layer at the Dead Sea, *Environmental Chemistry*, 12, 438, doi:10.1071/EN14224, 2015.
- Hönninger, G., Bobrowski, N., Palenque, E. R., Torrez, R., and Platt, U.: Reactive bromine and sulfur emissions at Salar de Uyuni, Bolivia, *Geophys. Res. Lett.*, 31, 4 PP., doi:10.1029/2003GL018818, 2004.
- Hörmann, C., Sihler, H., Bobrowski, N., Beirle, S., Penning de Vries, M., Platt, U., and Wagner, T.: Systematic investigation of bromine monoxide in volcanic plumes from space by using the GOME-2 instrument, *Atmos. Chem. Phys.*, 13, 4749–4781, doi:10.5194/acp-13-4749-2013, <http://www.atmos-chem-phys.net/13/4749/2013/>, 2013.
- Ingmann, P., Veihelmann, B., Straume, A., and Meijer, Y.: The status of implementation of the atmospheric composition related GMES missions Sentinel-4/Sentinel-5 and Sentinel-5p, Proceedings of the 2012 EUMETSAT Meteorological Satellite Conference, Sopot, Poland, Sept. 3-7, 2012. 🏔️

- Joiner, J., Vasilkov, A., Flittner, D., Buscela, E., and Gleason, J.: Retrieval of Cloud Pressure from Rotational Raman Scattering, Chapter 3 in: OMI Algorithm Theoretical Basis Document, Volume III - Clouds, Aerosols, and Surface UV Irradiance, Version 2.0, pp. P. 31–46, available at: <http://eosps0.gsfc.nasa.gov/sites/default/files/atbd/ATBD-OMI-03.pdf>; last access on 28 January 2016, 2002.
- KNMI: Background information about the Row Anomaly in OMI, <http://www.knmi.nl/omi/research/product/rowanomaly-background.php>, last access on 28 January 2016, 2015.
- Koelemeijer, R. B. A. and Stammes, P.: A fast method for retrieval of cloud parameters using oxygen A band measurements from the Global Ozone Monitoring Experiment, *J. Geophys. Res.*, 106, 3475–3490, doi:10.1029/2000JD900657, 2001.
- Koelemeijer, R. B. A., Stammes, P., Hovenier, J. W., and de Haan, J. F.: Global distributions of effective cloud fraction and cloud top pressure derived from oxygen A band spectra measured by the Global Ozone Monitoring Experiment: Comparison to ISCCP data, *J. Geophys. Res.*, 107, AAC 5–1, doi:10.1029/2001JD000840, 2002.
- Leser, H., Hönninger, G., and Platt, U.: MAX–DOAS measurements of BrO and NO₂ in the marine boundary layer, *Geophys. Res. Lett.*, 30, 4 PP., doi:10.1029/2002GL015811, 2003.
- Levelt, P. F., van den Oord, G. H. J., Dobber, M. R., Mälkki, A., Visser, H., de Vries, J., Stammes, P., Lundell, J. O. V., and Saari, H.: The Ozone Monitoring Instrument, *IEEE Trans. Geosci. Remote Sens.*, 44, 1093–1101, 2006.
- Lieb-Lappen, R. M. and Obbard, R. W.: The role of blowing snow in the activation of bromine over first-year Antarctic sea ice, *Atmospheric Chemistry and Physics*, 15, 7537–7545, doi:10.5194/acp-15-7537-2015, 2015.
- Loyola R., D. G.: Automatic cloud analysis from polar-orbiting satellites using neural network and data fusion techniques, vol. 4, pp. 2530–2533, IEEE, doi:10.1109/IGARSS.2004.1369811, 2004.
- Lübcke, P., Bobrowski, N., Arellano, S., Galle, B., Garzón, G., Vogel, L., and Platt, U.: BrO/SO₂ molar ratios from scanning DOAS measurements in the NOVAC network, *Solid Earth*, 5, 409–424, doi:10.5194/se-5-409-2014, 2014.
- Martin, M., Pöhler, D., Seitz, K., Sinreich, R., and Platt, U.: BrO measurements over the Eastern North–Atlantic, *Atmospheric Chemistry and Physics*, 9, 9545–9554, doi:10.5194/acp-9-9545-2009, 2009.
- Matveev, V., Peleg, M., Rosen, D., Tov-Alper, D. S., Hebestreit, K., Stutz, J., Platt, U., Blake, D., and Luria, M.: Bromine oxide—ozone interaction over the Dead Sea, *Journal of Geophysical Research: Atmospheres*, 106, 10 375–10 387, doi:10.1029/2000JD900611, 2001.
- Mehta, A. S., Ghosh, P. K., Shah, H. N., and Sanghavi, R. J.: Ideas for process improvement emanating from audit of a bromine plant in the Greater Rann of Kutch, *Indian J. Chem. Technol.*, 10, pp. 644–653, 2003.
- Munro, R., Eisinger, M., Anderson, C., Callies, J., Carpaccioli, E., Lang, R., Lefevre, A., Livschitz, Y., and Albinana, A. P.: GOME-2 on MetOp, The 2006 EUMETSAT Meteorological Satellite Conference, Helsinki, Finland, 2006.
- Oltmans, S. J.: Surface ozone measurements in clean air, *Journal of Geophysical Research*, 86, 1174, doi:10.1029/JC086iC02p01174, 1981.
- Oltmans, S. J. and Komhyr, W. D.: Surface ozone distributions and variations from 1973–1984: Measurements at the NOAA Geophysical Monitoring for Climatic Change Baseline Observatories, *Journal of Geophysical Research*, 91, 5229, doi:10.1029/JD091iD04p05229, 1986.
- Oppenheimer, C., Tsanev, V., Braban, C., Cox, R., Adams, J., Aiuppa, A., Bobrowski, N., Delmelle, P., Barclay, J., and Mcgonigle, A.: BrO formation in volcanic plumes, *Geochim. Cosmochim. Ac.*, 70, 2935–2941, doi:10.1016/j.gca.2006.04.001, 2006.
- Pacha, F.: My Name is Salt - a documentary film by Farida Pacha, trigon-film, Ennetbaden, Switzerland, <http://mynameissalt.com>, available on DVD after 28th February 2015, OV with subtitles: english, français, german, 2013. 

- Peterson, P. K., Simpson, W. R., Pratt, K. A., Shepson, P. B., Frieß, U., Zielcke, J., Platt, U., Walsh, S. J., and Nghiem, S. V.: Dependence of the vertical distribution of bromine monoxide in the lower troposphere on meteorological factors such as wind speed and stability, *Atmospheric Chemistry and Physics*, 15, 2119–2137, doi:10.5194/acp-15-2119-2015, 2015.
- Platt, U. and Janssen, C.: Observation and role of the free radicals NO₃, ClO, BrO and IO in the troposphere, *Faraday Discussions*, 100, 175, doi:10.1039/fd9950000175, 1995.
- Platt, U. and Lehrer, E.: Arctic Tropospheric Ozone Chemistry (ARCTOC) - Results from field, laboratory and modelling studies, Final Report of the EU-Project EV5V-CT93-0318, available online via <http://bookshop.europa.eu/en/arctic-tropospheric-ozone-chemistry-pbCGNA17783/>, last access on 28 January 2016, 1997.
- Platt, U. and Stutz, J.: Differential Optical Absorption Spectroscopy: Principles And Applications, Springer, 2008.
- 10 Pöhler, D., Vogel, L., Friess, U., and Platt, U.: Observation of halogen species in the Amundsen Gulf, Arctic, by active long-path differential optical absorption spectroscopy, *Proceedings of the National Academy of Sciences*, 107, 6582–6587, doi:10.1073/pnas.0912231107, 2010.
- Read, K. A., Mahajan, A. S., Carpenter, L. J., Evans, M. J., Faria, B. V. E., Heard, D. E., Hopkins, J. R., Lee, J. D., Moller, S. J., Lewis, A. C., Mendes, L., McQuaid, J. B., Oetjen, H., Saiz-Lopez, A., Pilling, M. J., and Plane, J. M. C.: Extensive halogen-mediated ozone destruction over the tropical Atlantic Ocean, *Nature*, 453, 1232–1235, doi:10.1038/nature07035, 2008.
- 15 Richter, A., Wittrock, F., Eisinger, M., and Burrows, J. P.: GOME observations of tropospheric BrO in northern hemispheric spring and summer 1997, *Geophysical Research Letters*, 25, 2683–2686, doi:10.1029/98GL52016, 1998.
- Rix, M., Valks, P., Hao, N., Loyola, D., Schlager, H., Huntrieser, H., Flemming, J., Koehler, U., Schumann, U., and Inness, A.: Volcanic SO₂, BrO and plume height estimations using GOME-2 satellite measurements during the eruption of Eyjafjallajökull in May 2010, *J. Geophys. Res.*, 117, doi:10.1029/2011JD016718, 2012.
- 20 Rozanov, V. V., Kokhanovsky, A. A., Loyola, D., Siddans, R., Latter, B., Stevens, A., and Burrows, J. P.: Intercomparison of cloud top altitudes as derived using GOME and ATSR-2 instruments onboard ERS-2, *Remote Sensing of Environment*, 102, 186–193, doi:10.1016/j.rse.2006.02.009, 2006.
- Saiz-Lopez, A.: Bromine oxide in the mid-latitude marine boundary layer, *Geophysical Research Letters*, 31, doi:10.1029/2003GL018956, 2004.
- 25 Saiz-Lopez, A. and von Glasow, R.: Reactive halogen chemistry in the troposphere, *Chem. Soc. Rev.*, 41, 6448–6472, doi:10.1039/C2CS35208G, 2012.
- Salawitch, R. J., Canty, T., Kurosu, T., Chance, K., Liang, Q., da Silva, A., Pawson, S., Nielsen, J. E., Rodriguez, J. M., Bhartia, P. K., Liu, X., Huey, L. G., Liao, J., Stickel, R. E., Tanner, D. J., Dibb, J. E., Simpson, W. R., Donohoue, D., Weinheimer, A., Flocke, F., Knapp, D., Montzka, D., Neuman, J. A., Nowak, J. B., Ryerson, T. B., Oltmans, S., Blake, D. R., Atlas, E. L., Kinnison, D. E., Tilmes, S.,
- 30 Pan, L. L., Hendrick, F., Van Roozendaal, M., Kreher, K., Johnston, P. V., Gao, R. S., Johnson, B., Bui, T. P., Chen, G., Pierce, R. B., Crawford, J. H., and Jacob, D. J.: A new interpretation of total column BrO during Arctic spring, *Geophys. Res. Lett.*, 37, L21 805, doi:10.1029/2010GL043798, <http://onlinelibrary.wiley.com/doi/10.1029/2010GL043798/abstract>, 2010.
- Sihler, H., Platt, U., Beirle, S., Marbach, T., Kühl, S., Dörner, S., Verschaeve, J., Frieß, U., Pöhler, D., Vogel, L., Sander, R., and Wagner, T.: Tropospheric BrO column densities in the Arctic derived from satellite: retrieval and comparison to ground-based measurements, *Atmos. Meas. Tech.*, 5, 2779–2807, doi:10.5194/amt-5-2779-2012, 2012.
- Smoydzin, L. and von Glasow, R.: Modelling chemistry over the Dead Sea: bromine and ozone chemistry, *Atmospheric Chemistry and Physics*, 9, 5057–5072, doi:10.5194/acp-9-5057-2009, 2009.

- Stammes, P., Sneep, M., de Haan, J. F., Veefkind, J. P., Wang, P., and Levelt, P. F.: Effective cloud fractions from the Ozone Monitoring Instrument: Theoretical framework and validation, *J. Geophys. Res.*, 113, D16S38, doi:10.1029/2007JD008820, <http://onlinelibrary.wiley.com/doi/10.1029/2007JD008820/abstract>, 2008.
- Stutz, J., Ackermann, R., Fast, J. D., and Barrie, L.: Atmospheric reactive chlorine and bromine at the Great Salt Lake, Utah, *Geophysical Research Letters*, 29, 18–1–18–4, doi:10.1029/2002GL014812, 2002.
- Tas, E., Peleg, M., Matveev, V., Zingler, J., and Luria, M.: Frequency and extent of bromine oxide formation over the Dead Sea, *Journal of Geophysical Research: Atmospheres*, 110, doi:10.1029/2004JD005665, 2005.
- Tas, E., Peleg, M., Pedersen, D. U., Matveev, V., Pour Biazar, A., and Luria, M.: Measurement-based modeling of bromine chemistry in the boundary layer: 1. Bromine chemistry at the Dead Sea, *Atmospheric Chemistry and Physics*, 6, 5589–5604, doi:10.5194/acp-6-5589-2006, 2006.
- Theys, N., Roozendael, M. V., Dils, B., Hendrick, F., Hao, N., and Mazière, M. D.: First satellite detection of volcanic bromine monoxide emission after the Kasatochi eruption, *Geophys. Res. Lett.*, 36, 4 PP., doi:200910.1029/2008GL036552, 2009a.
- Theys, N., Van Roozendael, M., Errera, Q., Hendrick, F., Daerden, F., Chabrillat, S., Dorf, M., Pfeilsticker, K., Rozanov, A., Lotz, W., Burrows, J. P., Lambert, J.-C., Goutail, F., Roscoe, H. K., and De Mazière, M.: A global stratospheric bromine monoxide climatology based on the BASCOE chemical transport model, *Atmos. Chem. Phys.*, 9, 831–848, 2009b.
- Theys, N., Van Roozendael, M., Hendrick, F., Yang, X., De Smedt, I., Richter, A., Begoin, M., Errera, Q., Johnston, P. V., Kreher, K., and De Mazière, M.: Global observations of tropospheric BrO columns using GOME-2 satellite data, *Atmos. Chem. Phys.*, 11, 1791–1811, 2011.
- Theys, N., De Smedt, I., Van Roozendael, M., Froidevaux, L., Clarisse, L., and Hendrick, F.: First satellite detection of volcanic OCIO after the eruption of Puyehue-Cordón Caulle, *Geophys. Res. Lett.*, 41, 667–672, doi:10.1002/2013GL058416, 2014.
- Torres, O., Tanskanen, A., Veihelmann, B., Ahn, C., Braak, R., Bhartia, P. K., Veefkind, P., and Levelt, P.: Aerosols and surface UV products from Ozone Monitoring Instrument observations: An overview, *J. Geophys. Res.*, 112, D24S47, doi:10.1029/2007JD008809, <http://onlinelibrary.wiley.com/doi/10.1029/2007JD008809/abstract>, 2007.
- Vandaele, A. C., Hermans, C., Fally, S., Carleer, M., Colin, R., Mérienne, M., Jenouvrier, A., and Coquart, B.: High-resolution Fourier transform measurement of the NO₂ visible and near-infrared absorption cross sections: Temperature and pressure effects, *Journal of Geophysical Research*, 107, 12 PP., doi:200210.1029/2001JD000971, 2002.
- Vasilkov, A., Joiner, J., Spurr, R., Bhartia, P. K., Levelt, P., and Stephens, G.: Evaluation of the OMI cloud pressures derived from rotational Raman scattering by comparisons with other satellite data and radiative transfer simulations, *J. Geophys. Res.*, 113, D15S19, doi:10.1029/2007JD008689, <http://onlinelibrary.wiley.com/doi/10.1029/2007JD008689/abstract>, 2008.
- Veefkind, J. P., Aben, I., McMullan, K., Förster, H., de Vries, J., Otter, G., Claas, J., Eskes, H. J., de Haan, J. F., Kleipool, Q., van Weele, M., Hasekamp, O., Hoogeveen, R., Landgraf, J., Snel, R., Tol, P., Ingmann, P., Voors, R., Kruizinga, B., Vink, R., Visser, H., and Levelt, P. F.: TROPOMI on the ESA Sentinel-5 Precursor: A GMES mission for global observations of the atmospheric composition for climate, air quality and ozone layer applications, *Remote Sensing of Environment*, 120, 70–83, doi:10.1016/j.rse.2011.09.027, 2012.
- Wagner, T. and Platt, U.: Satellite mapping of enhanced BrO concentrations in the troposphere, *Nature*, 395, 486–490, doi:10.1038/26723, 1998.
- Wagner, T., Beirle, S., and Deutschmann, T.: Three-dimensional simulation of the Ring effect in observations of scattered sun light using Monte Carlo radiative transfer models, *Atmos. Meas. Tech.*, 2, 113–124, doi:10.5194/amt-2-113-2009, 2009.

Wilmouth, D. M., Hanisco, T. F., Donahue, N. M., and Anderson, J. G.: Fourier Transform Ultraviolet Spectroscopy of the $A^2\Pi_{3/2} \leftarrow X^2\Pi_{3/2}$ Transition of BrO, J. Phys. Chem. A, 103, 8935–8945, doi:10.1021/jp991651o, 1999.

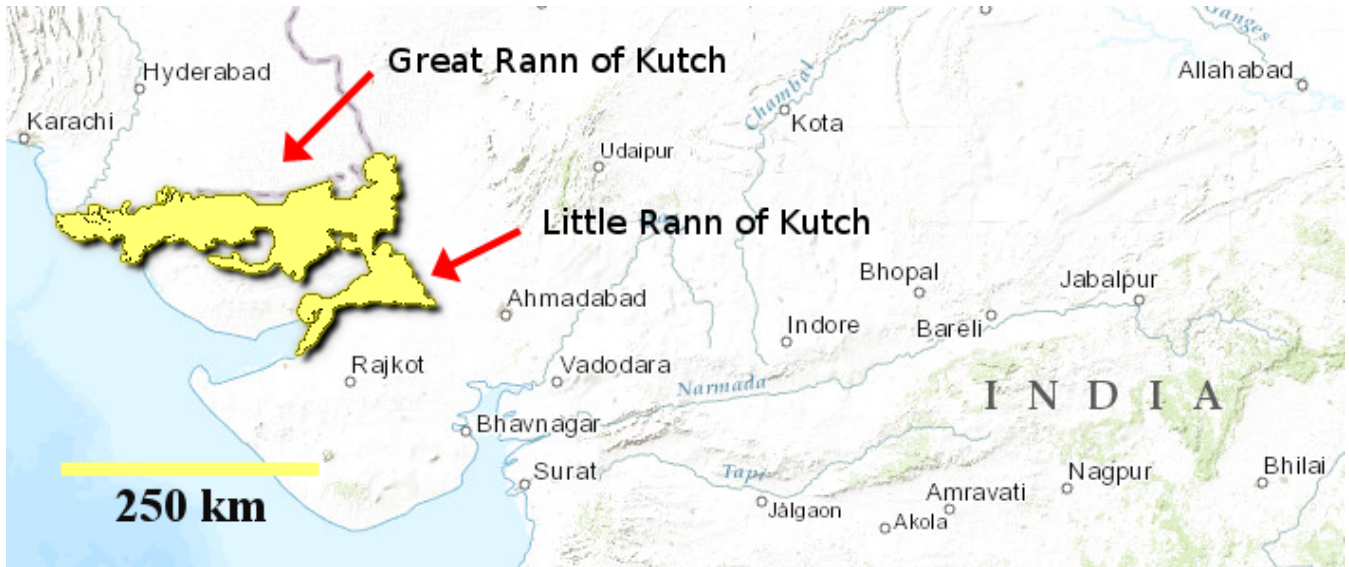


Figure 1. Location of the Great and Little Rann of Kutch. While about 10% of the Great Rann belong to Pakistan, the main part as well as the Little Rann are located in the Kutch District of Gujarat, India (adapted from **World Wildlife Fund:** Rann of Kutch seasonal salt marsh, 2014. Retrieved from <http://www.eoearth.org/view/article/155658>, last access on 28 January 2016, CC BY-SA 2.5).

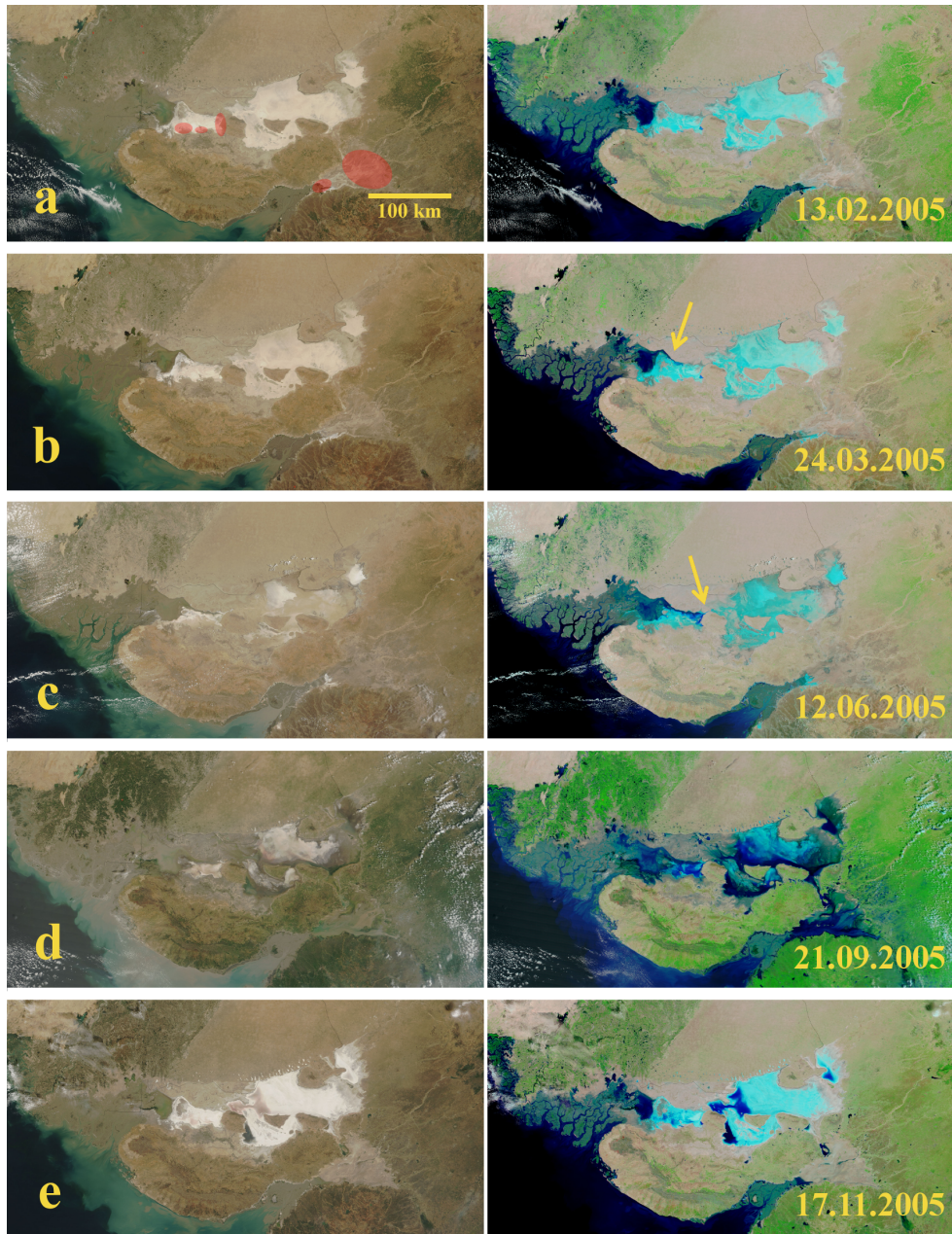


Figure 2. MODIS true color (TC, left) and Band 7-2-1 images (right) over the Rann of Kutch for selected days in a) February, b) March, c) June, d) September and e) November 2005 (13.2., 24.3. 12.6., 21.9. and 17.11.), illustrating the flood during the monsoon. Water can be identified from the 7-2-1 images as dark blue/black, while clouds and bright surfaces appear light blue. The Rann appears as a bright surface earlier the year, before it darkens due to inflowing water (indicated by yellow arrows in b) and c), right column; compare with the mean reflectivity shown in Figure 4). During monsoon time, the entire Rann is often completely flooded and large areas are dominated by mud (TC image in September). Locations of industrial evaporation ponds are indicated by red marked areas in a).

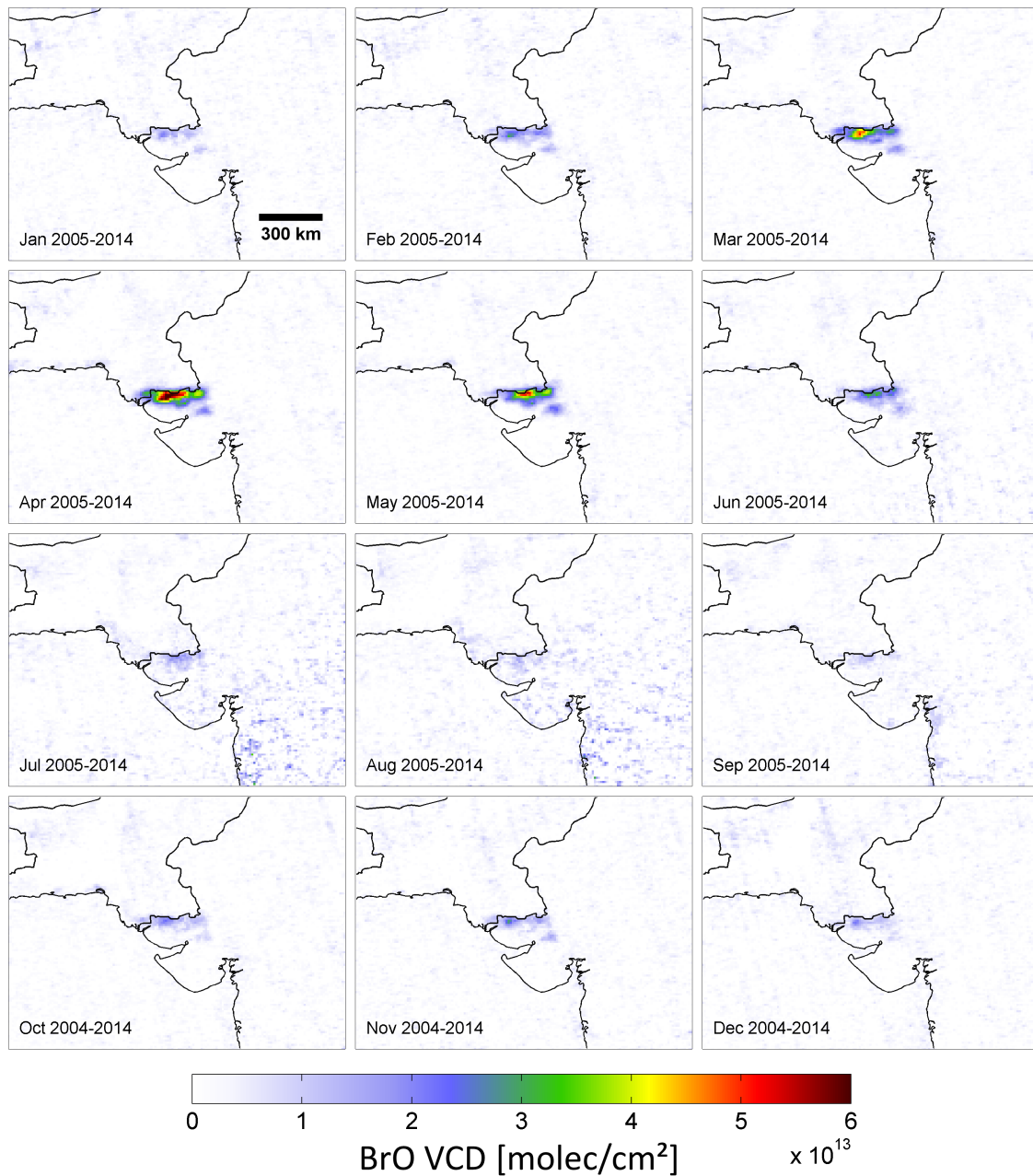


Figure 3. Seasonal variation of monthly mean BrO VCDs with CF<30% over the Rann of Kutch as seen by OMI during 2004-2014. While maximum VCDs are clearly detected in April/May for the Great and Little Rann, only small enhancements can be seen during wintertime. Results during the monsoon season (July–September) include less measurements due to increased cloud frequency leading to a higher noise level, especially in the south-eastern part of the shown region. Please note that OMI data are only available since October 2004, i.e. no data for January–September 2004 are included.

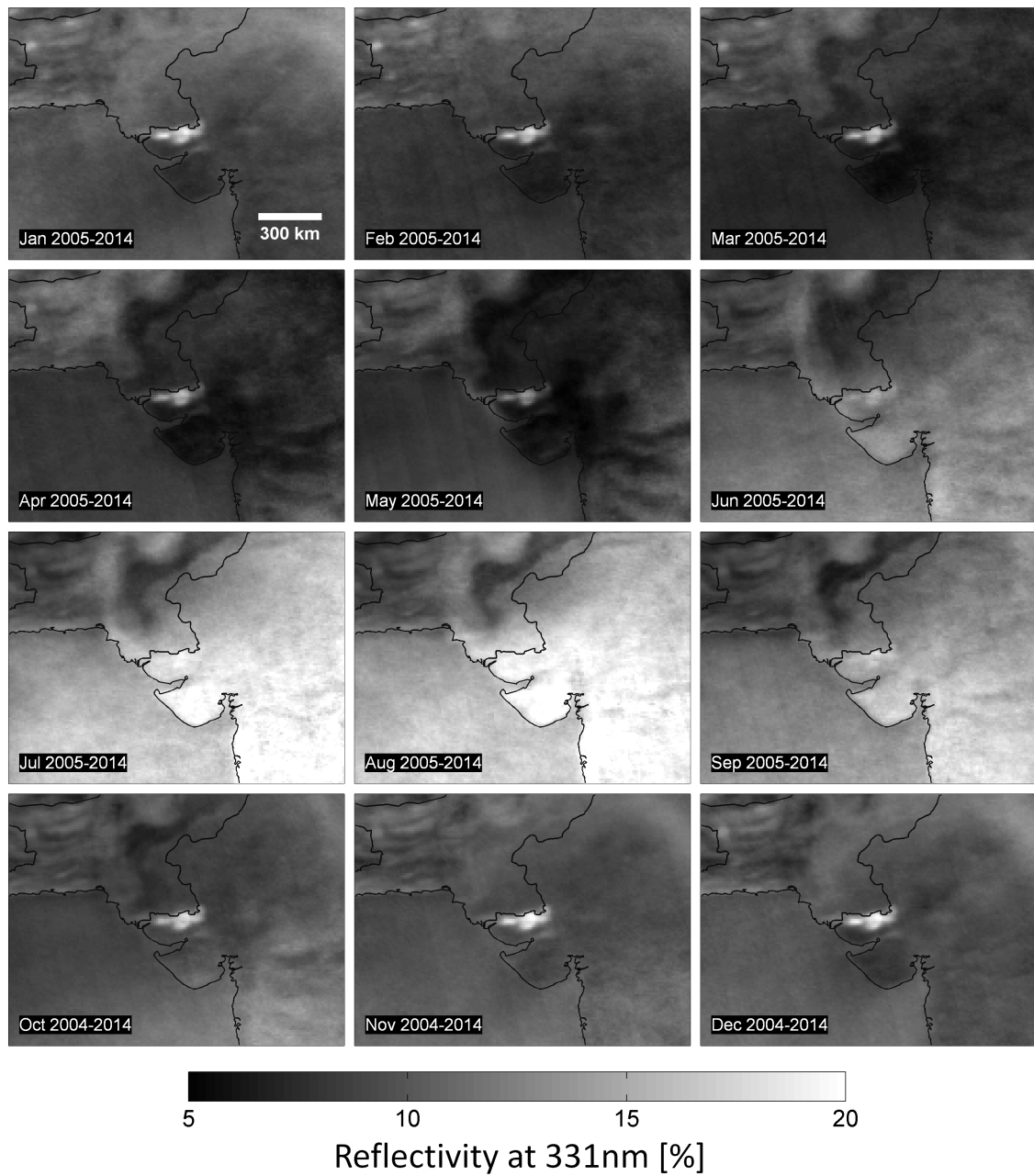


Figure 4. Seasonal variation of the monthly mean reflectivity at 331 nm over the Rann of Kutch as seen by OMI during 2004-2014 (same data selection as in Figure 3, i.e. for $CF < 0.3$). Only the Great Rann of Kutch can be clearly identified due to its bright surface compared to the surrounding areas. During the monsoon (July–September), wide areas are still affected by clouds as indicated by the increased background, including the Rann area. It is important to note that enhanced BrO VCDs in Figure 3 appear only at certain parts of the salt marsh (area of enhanced reflectivity) and especially for rather low reflectivity in April/May.

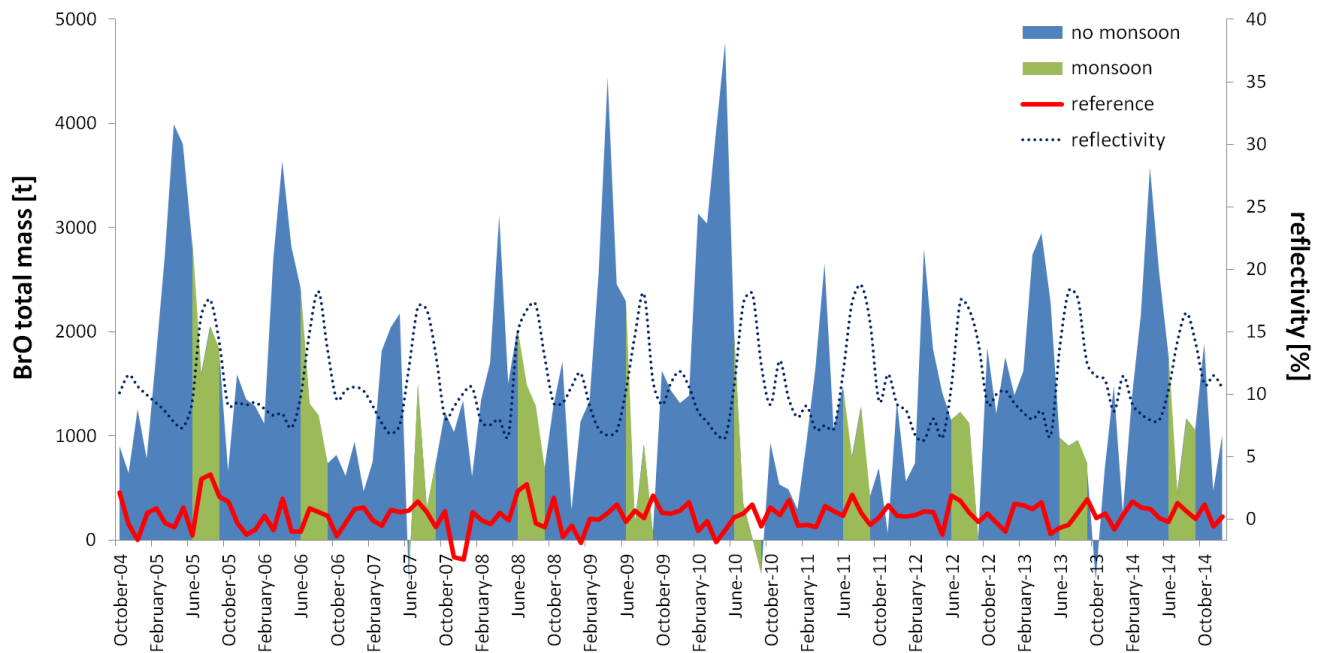


Figure 5. Total BrO mass over the Rann of Kutch area calculated from monthly averaged BrO VCD OMI data for the baseline scenario (i.e. a homogeneous layer reaching from the surface up to 1 km) from October 2004 until December 2014. During monsoon months (green) the reflectivity (blue dotted line) shows maximum values due to cloud coverage, while the BrO mass is lowered (partly due to cloud shielding). Maximum BrO masses are typically accompanied by a rather low reflectivity. For comparison, BrO masses obtained over a corresponding reference area of the same size directly west of the considered region are indicated by the red line.

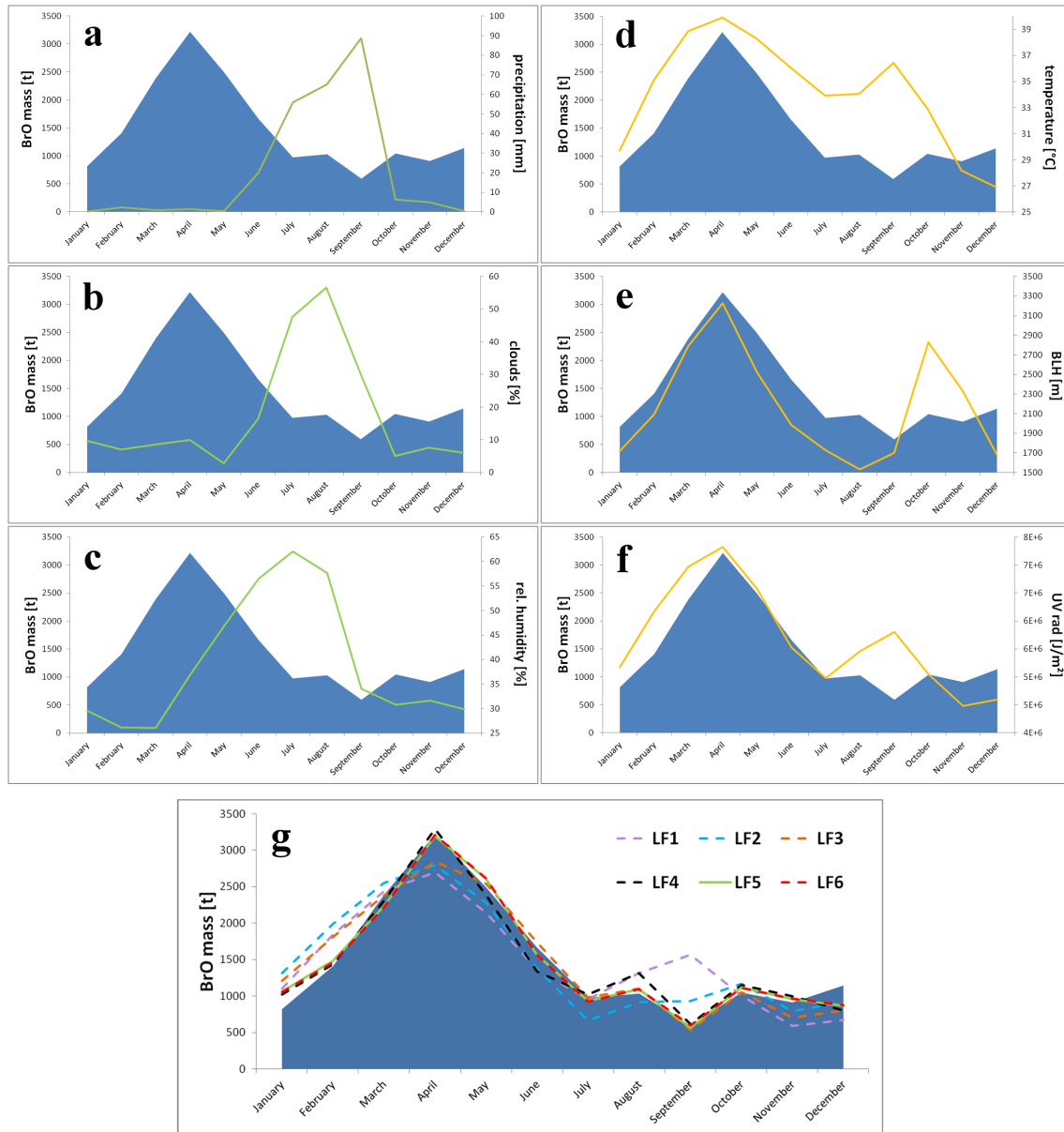


Figure 6. Monthly averaged variation of ECMWF meteorological parameters (thin lines) in comparison to the total BrO mass (blue area) over the Rann of Kutch during 2004-2014. The parameters can be divided into two groups by their seasonal behaviour (precipitation, cloud coverage and relative humidity are shown within the left column in green, **a–c**; surface temperature, boundary layer height and UV radiation within the right column in orange, **d–f**). The latter mentioned parameters correlate very well with the BrO mass during the first half-year, before a second maximum shows up after the end of the monsoon. The results of a multilinear regression analysis suggest that a simple linear model (linear functions LF1–LF6, **g**) can be used to adequately describe the annual variations (see text and Table 2 for further details).

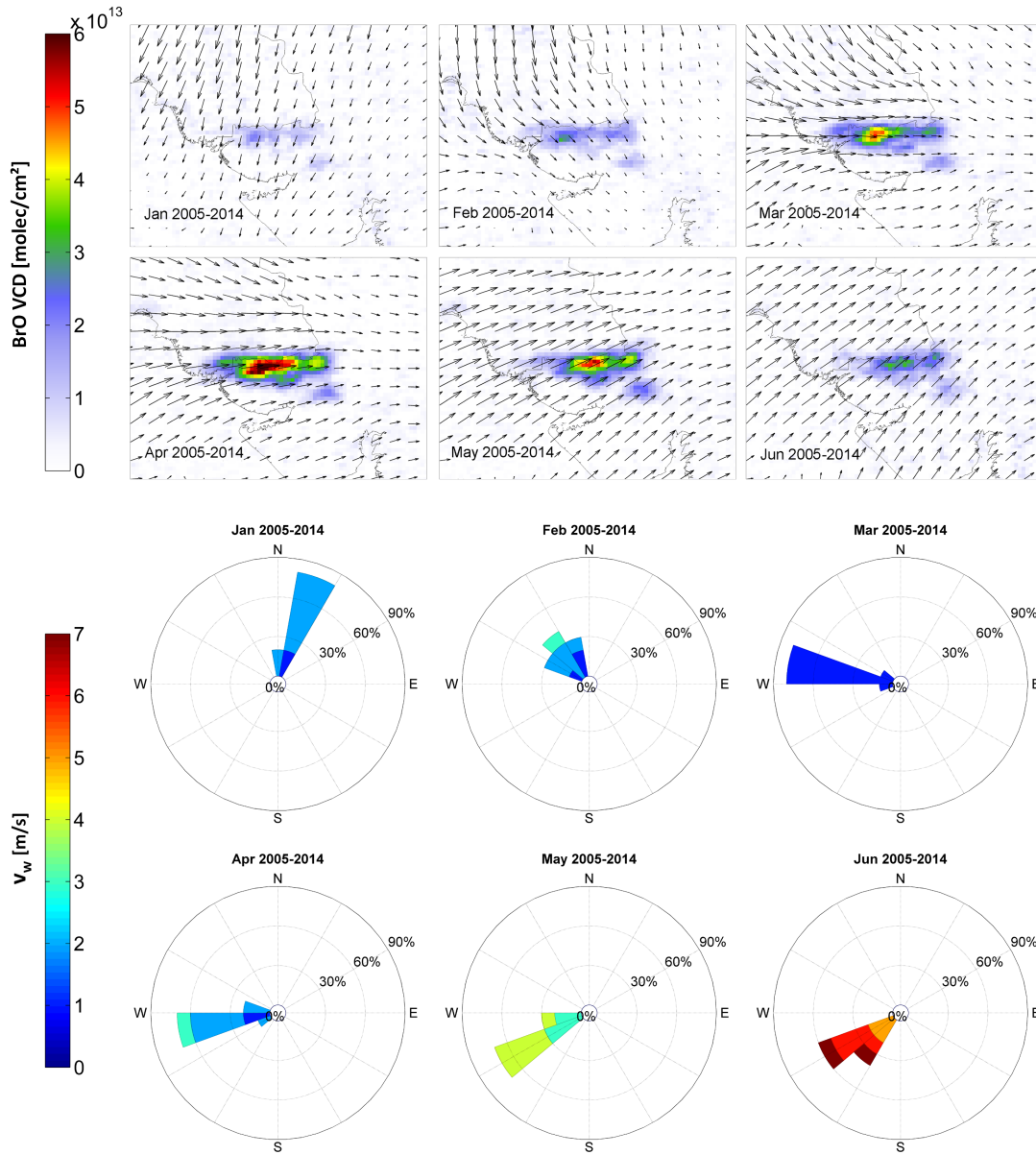



Figure 7. Mean wind field at 10 m altitude over the Rann of Kutch for the time around the OMI overpass (9 UTC) during January–June 2005–2014 according to ECMWF data together with the BrO VCDs observed from OMI (upper panel). The area is mainly affected by westerly winds at times when BrO VCDs are high. A shift of the BrO distribution in May can be explained by a turning of the main wind direction (and increasing velocity) towards north-east. Corresponding wind speeds (lower panels) are rather low (1-3 m/s) before they increase with the onset of the monsoon season (>7 m/s) 

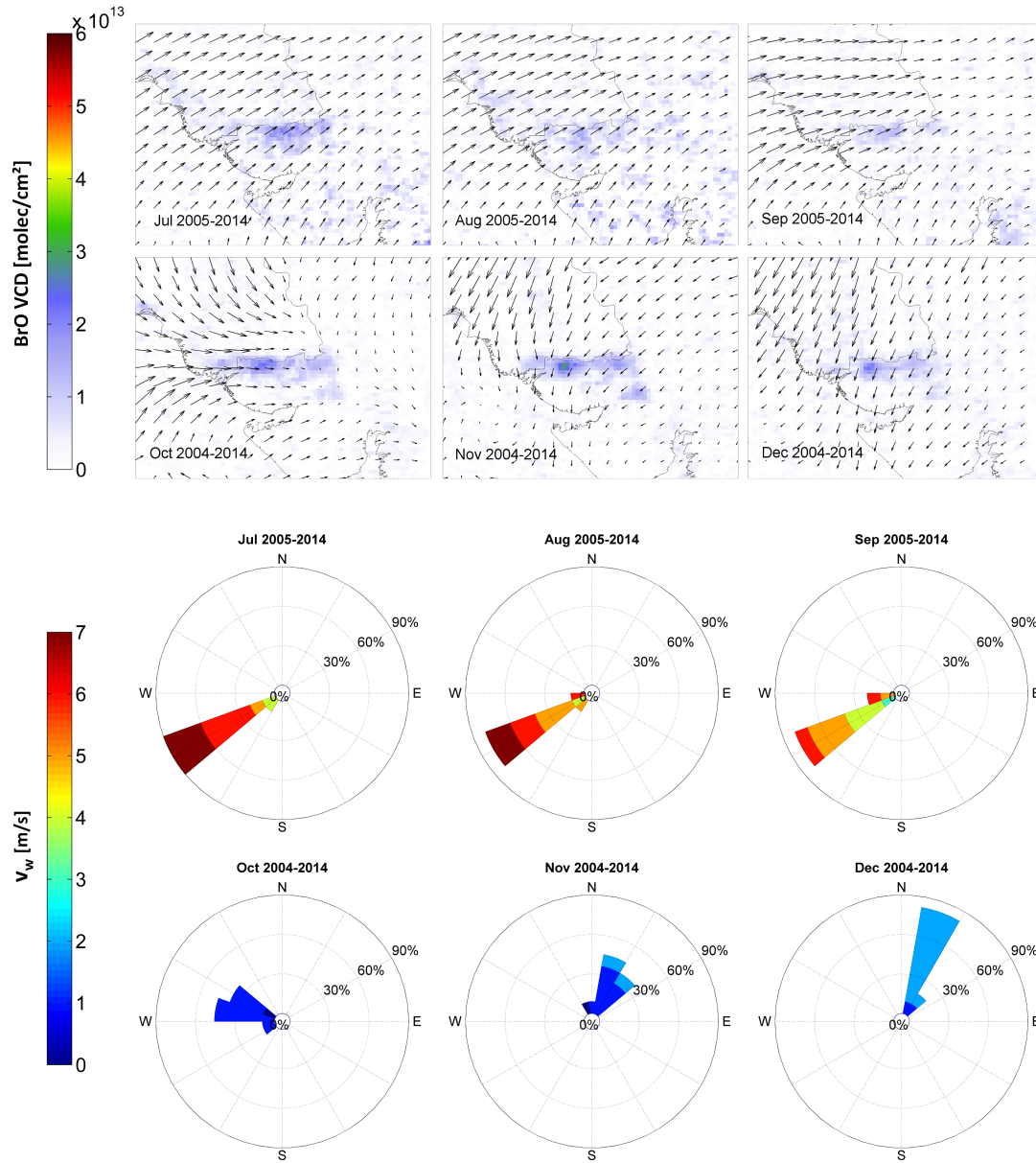


Figure 8. Same as in Figure 7, but for July to December 2004–2014. The area is mainly affected by strong southwestern winds during monsoon months (>7 m/s). After the monsoon, the wind speed rapidly drops (≈ 2 m/s) and the wind direction changes from west (October) to northeast during wintertime.

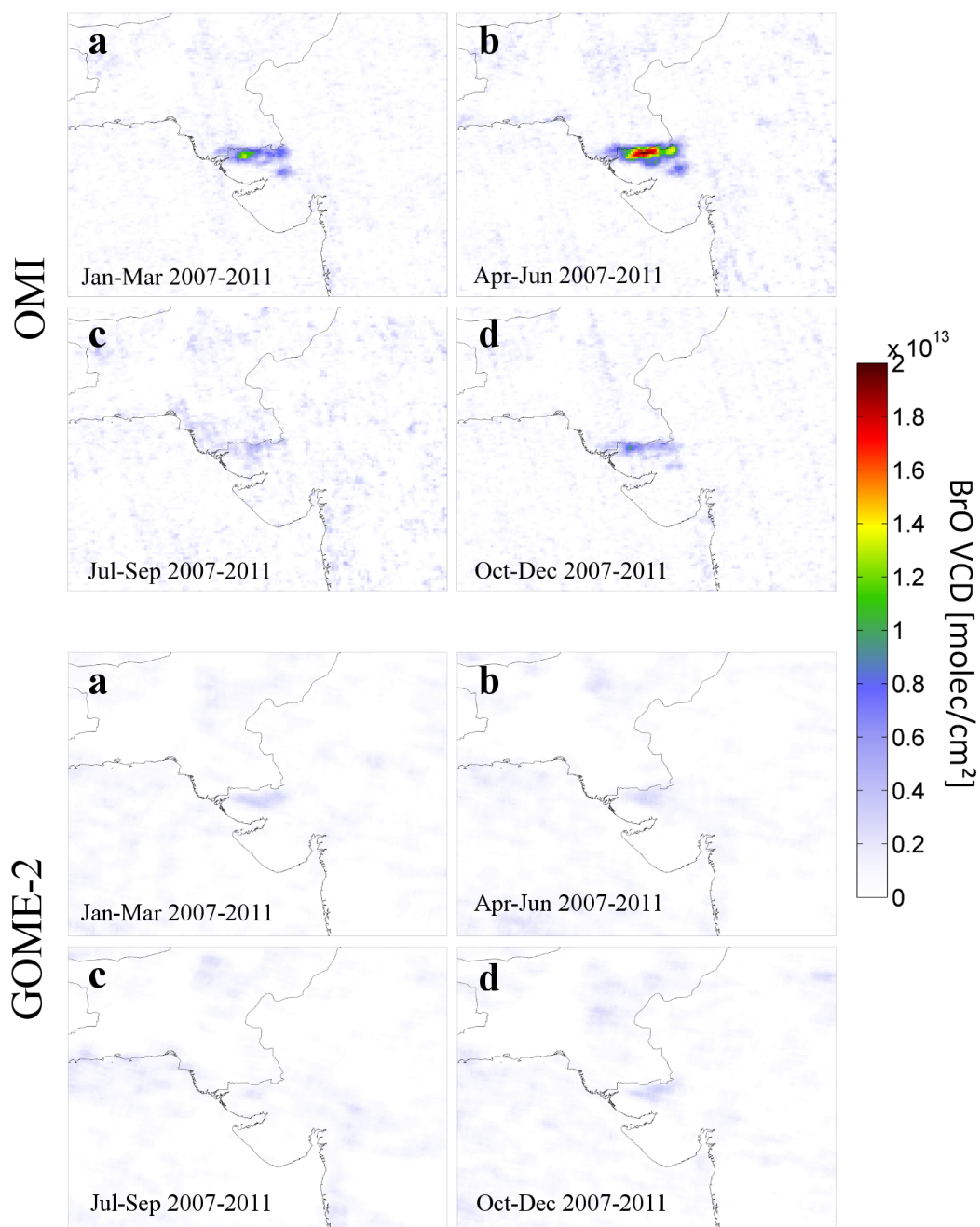


Figure 9. Seasonal mean BrO VCDs over the Rann of Kutch area for OMI (upper panel) and GOME-2 (lower panel) in 2007-2011: **a)** January–March, **b)** April–June, **c)** July–September, **d)** October–December. Even for the largest BrO VCDs as seen by OMI during April–June, the GOME-2 VCDs are close to the detection limit and might be at least partly explained by retrieval artefacts caused by the bright surface. Note that, in contrast to Figure 3, no cloud filter was applied (see text).

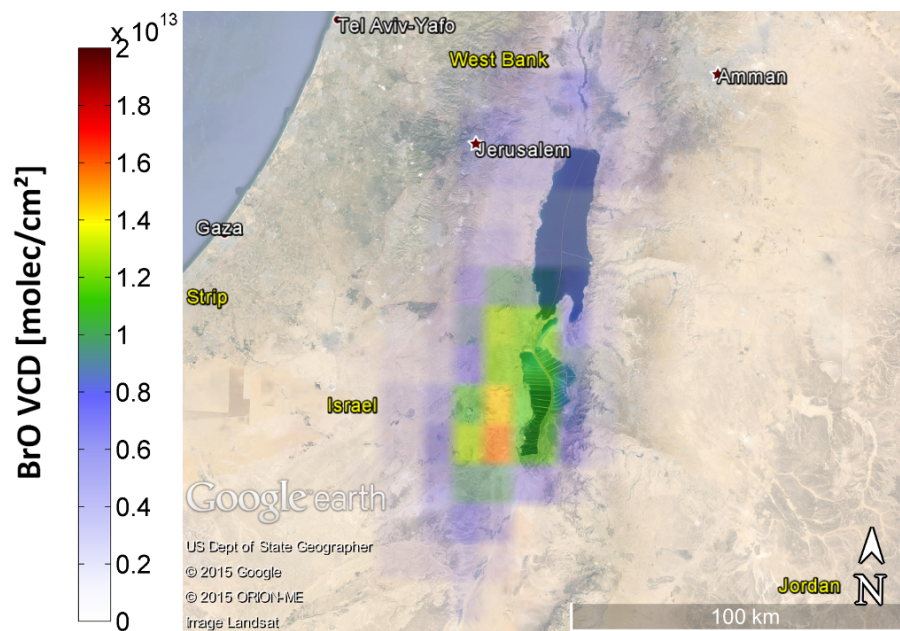


Figure 10. Averaged BrO VCDs over the Dead Sea as seen by OMI during summer months 2005-2014 (April–October). A clear BrO enhancement can be seen over the southern part of the Dead Sea, confirming former ground-based observations by (Hebestreit et al., 1999), (Matveev et al., 2001) and (Tas et al., 2005).

Table 1. Uncertainty of BrO mixing ratio estimation based on the variation of assumed properties (BrO profile, surface albedo, aerosol optical density) for the AMF calculation. (*) AOD=0 corresponds to a non-aerosol scenario.

a priori	baseline	alternatives	mixing ratio [ppt]	ΔBrO [%]
layer profile	0–1 km	0–400 m	$(47\pm13)\text{ppt}$	+34%
		0–2 km	$(27\pm8)\text{ppt}$	-23%
AOD	0.7	0*	$(32\pm9)\text{ppt}$	-8%
		0.4	$(34\pm10)\text{ppt}$	-3%
		1.0	$(37\pm11)\text{ppt}$	+6%
surface albedo	0.15	0.1	$(42\pm12)\text{ppt}$	+20%
		0.2	$(30\pm9)\text{ppt}$	-14%

Table 2. Best fits from the multilinear regression analysis in order to model the seasonal BrO mass variation over the Rann of Kutch in dependency of UV surface radiation (UV), precipitation (P), cloud coverage (CC), relative humidity (RH), boundary layer height (BLH) and surface temperature (T).

#	linear function	r^2
1	$m_{BrO} = a_1 \cdot UV$	0.71
2	$m_{BrO} = a_1 \cdot UV + a_2 \cdot P$	0.83
3	$m_{BrO} = a_1 \cdot UV + a_2 \cdot P + a_4 \cdot RH$	0.91
4	$m_{BrO} = a_1 \cdot UV + a_3 \cdot CC + a_4 \cdot RH + a_5 \cdot BLH$	0.95
5	$m_{BrO} = a_1 \cdot UV + a_2 \cdot P + a_3 \cdot CC + a_4 \cdot RH + a_5 \cdot BLH$	0.97
6	$m_{BrO} = a_1 \cdot UV + a_2 \cdot P + a_3 \cdot CC + a_4 \cdot RH + a_5 \cdot BLH + a_6 \cdot T$	0.97